Effect of High Frequency Harmonics on High Voltage Insulation

Shruti Seshadri

TU Delft

Effect of High Frequency Harmonics on High Voltage Insulation

by

Shruti Seshadri

to obtain the degree of Master of Science

at the Delft University of Technology,

to be defended publicly on August 28th, 2020 at 09:00 AM.

Student number:	4850513	
Project duration:	December 12, 2019 – August 28, 2020	
Supervisors:	Prof. Ir. Peter Vaessen,	Dr. Mohamad Ghaffarian. Niasar
Thesis committee:	Prof. Ir. Peter Vaessen,	TU Delft, supervisor
	Dr. Mohamad Ghaffarian. Niasar,	TU Delft
	Dr. Patrizio Manganiello,	PVMD, TU Delft

TU Delft

Abstract

The Electricity distribution and generation is in a constant state of change. With the need to reduce our carbon emission and work towards a sustainable future, a large amount of time and money is being invested in the development of renewable energy sources. When these sources are connected to the grid, power electronic converters are involved. any sources such as solar PV, produce DC and hence need to be converted to AC. This reliance on power electronic and semiconductor devices leads to an influx of high frequency harmonics in the grid. According to a report published by the statistical office of the European Union, renewable energy's contribution to the gross final energy consumption has increased to 18%, which is double the share in 2004 (8.5%). By 2030, the EU aims to reach at least 32%. That being the case, in the near future, these high frequency harmonics and their effect on our power system is an increasing cause of concern. Equipment such as cables and transformers, that are currently being used are only tested for the fundamental frequency. Hence there is not much awareness regarding their behaviour to high frequency signals.

This is the problem that this thesis aims to resolve. With this thesis, high voltage insulation material will be tested under high voltage and high frequency signals to understand how the ageing is affected because of higher frequencies. The insulation samples were tested with a function generator and high voltage power amplifier till 1.6 kHz. However, the amplifier trips above this frequency and hence a more suitable method is discussed for a higher frequency range. A literature survey suggested the use of a series resonance circuit. This idea is studied by understanding the importance of inductor design and the effect of the resistance and capacitance that occur along with it. These parameters influence the functioning of an inductor and in turn, of the series resonance circuit. For this particular project when the series resonance circuit needs to operate at high frequency, the parasitic capacitance is often, a source of uncertainty. The measurement of parasitic capacitance is discussed in detail and different methods are also tried to obtain an accurate reading. It was understood that the parasitic capacitance is influenced by a number of factors, most of them being the geometry of the coil. Since measuring equipment also contain a certain amount of capacitance, this value must be measured very delicately and the

surrounding capacitance accounted for.

With the insulation samples tested using the high voltage power amplifier, the time to breakdown is noted by increasing the voltage gradually till it breaks down. This gives us the time and field strength at which the sample breaks down. The samples are also tested at successively lower voltages so that the life time curve of these insulation samples can be obtained. The results of these test have helped in understanding that at higher frequencies, the samples age faster. It is also possible to understand that the time to breakdown decreases as insulation sample is exposed to higher frequency signals. Studying the ageing of insulation under high frequency can lead to a more precise prediction of time of insulation failure and can prove to be a useful tool for planning in advance. Taking this research forward by creating a model which contains life time curves of different frequencies and a method to understand how these frequencies age the insulation when they occur together, will help the insulation failure prediction and analysis immensely.

Shruti Seshadri

Delft, August 23, 2020

Contents

1 Introduction **1**

1.1 The need for monitoring higher frequency signals . . . 1

1.2 Background research on transients and high frequency disturbances: . . . 2

1.3 Methods used to generate High frequency . . . 5

1.4 Goals of research. . . . 8

1.5 Thesis Layout . . . 9

2 Series Resonance Circuit Design **11**

3 Inductor Design **15**

3.1 Inductance . . . 15

3.2 Lumped Parameter representation of Inductor . . . 18

3.2.1 Parasitic Capacitance . . . 20

3.2.2 Resistive losses . . . 25

4 Parasitic capacitance and its Measurement **27**

4.1 Methods of verifying capacitance . . . 27

4.1.1 Through calculation from equations: . . . 28

4.1.2 Through COMSOL-Multiphysics: . . . 31

4.1.3 Through Experimental measurement: . . . 33

4.2 Analysis . . . 38

5 Experimental Insulation Testing **41**

5.1 Test set up and Procedure: . . . 41

5.2 Breakdown testing: . . . 44

5.3 Life time testing: . . . 47

6 Results **49**

6.1 Insulation testing and time to breakdown . . . 49

6.1.1 Weibull analysis: . . . 49

6.1.2 Test Results and Discussion: . . . 50

6.2 Insulation testing conclusion: 56

7 Reflection **57**

8 Conclusion and Recommendation **59**

8.1 Conclusion: 60

8.2 Recommendation: 61

A Appendix-1 **63**

B Appendix-2 **67**

Bibliography **69**

1

Introduction

1.1. The need for monitoring higher frequency signals

With every passing day, we witness a new high in the global electric consumption. It is now our aim to shift more of this consumption to be full filled through renewable energy sources. However, even till a few years back (around 2016-2017) about 80% of the energy generation in the world was through fossil fuels [1]. With the quickly diminishing fossil fuels and the increasing carbon emission, this method of energy generation and consumption, in no way works towards a sustainable future. Currently, shifting towards renewable energy sources for our electricity needs is a great way to reduce our reliance on fossil fuels as well as to controlling carbon emission. Inclusion of renewable energy sources, however, increase our dependence on power electronic converters as they are used to connect these sources to the grid. Their switching, in combination with the passive elements of the system, create impulses somewhere in the range of 5kHz to 15kHz [2, 3]. The grid that is in use currently, operates with cables and transformers that have been designed and tested for 50Hz or 60Hz. Hence arises the question on their performance under these high frequency harmonics. The effect these harmonics might have on the insulation of these high voltage cables and transformers is unclear as there is no well-established method as yet, with which their lifetime can be predicted. Harmonics injected into the grid, are actually a combination of a

few different frequencies, in varying magnitudes. Hence each one affects and ages the insulation differently. Since it is certain that we will be looking at an increase in the reliance on renewable energy sources, it is important to understand the effect this will have on the entire grid to prevent unforeseen failures and defects. This is the reason why testing at higher frequencies should also be considered important.

For testing high voltage insulation at high frequency an acceptable method needs to be developed. The aim of this thesis was to contribute towards this purpose by deciding on a circuit to test insulation samples and observe the effect high frequency signals have on their ageing. The testing should be possible over a wide range of frequency and must also permit frequency variation. With this, at each frequency, the time to breakdown and the electric stress of the insulation material will be available. The initial idea of this thesis was to design a test set up which would enable us to test an insulation sample under high voltage (about 20 kV) through a range of frequency (approx 50Hz to 15kHz) so that we get the time to breakdown of the sample at different frequencies. In the course of understanding the necessities of this particular test set up, the frequency range mentioned was split, as the lower range (50 Hz -1 kHz) could be tested with a different set up compared to the higher range (2 kHz-15 kHz). For testing a higher range, a resonance circuit was considered and it was realized that a lot had to be understood and studied regarding a high voltage inductor to work with this circuit. Hence the focus was shifted to the inductor. With the arrival of COVID19 and the lockdown, most of the experimental work was also shifted to focus on literature survey and simulation analysis. This work is explained in chapter 2 and chapter 3.

1.2. Background research on transients and high frequency disturbances:

Before starting to design a circuit for testing high voltage insulation at high frequencies, it is important to look at the high frequency signals that are actually the reason behind this thesis. Although high frequency harmonics are increasing with the increase in power electronic converters, their affect on high voltage insulation is still not confirmed. There have been failures which are claimed to be a result of these harmonics. One reason for this is because the failure occurred in the part of the insulation, where no over voltages were predicted. These failures occurred, despite laboratory testing showing no unusual voltage distribution and the transformer proving more than sufficient to withstand impulse testing. The reason behind such failures was found out to be fast repetitive disturbances, which occurred because of self-resonance in the transformers[4, 5].

Initially, the main source of such high frequency disturbances was the self-resonance from the transformers, high voltage switch mode power supplies, over voltages due to switching operation in vacuum circuit breaker etc [6, 7]. For instance, one very frequently used example when it comes

to high frequency signals due to power electronic components is the repeated failure of high voltage cable termination at Eagle-pass substation in Texas, USA. The purpose was to connect the US transmission grid to the Mexican transmission grid [8]. IGBT based Voltage Source Converters were used for PWM generation and hence for inversion. However, the high frequency harmonics generated due to the switching of converters create sites of local resonance leading to harmonics with increased amplitude. The predicted insulation life time was about 30 years, which was reduced to a few days because of the failures. There were certain harmonics, such as the 3rd and 21st which were predicted and were damped using RC filters. However, the presence of 207th harmonic which occurred at about 12.4 kHz, was not known and the magnitude also went to 40% of the power frequency voltage.

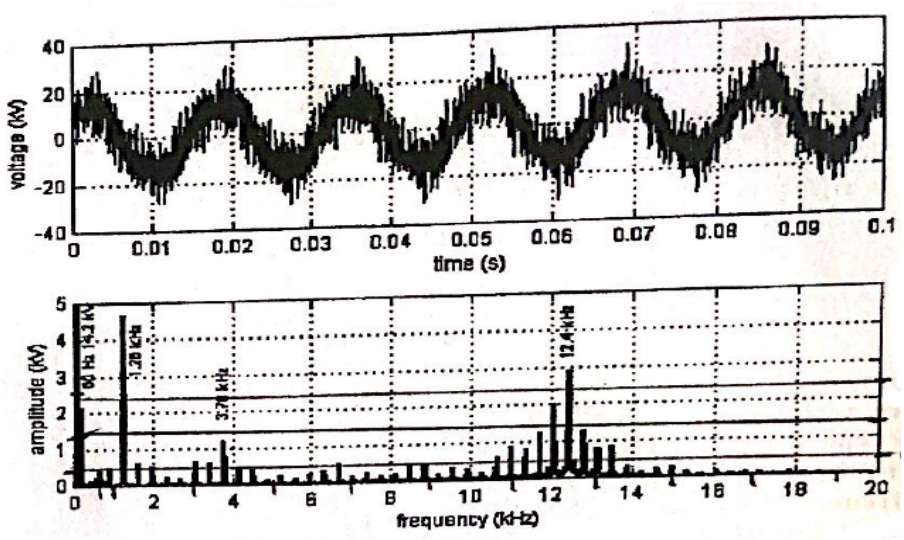

Figure 1.1: Voltage on the Mexican side of the eagle pass substation; Voltage waveform(above) , Harmonic spectrum average over 1 minute (below)[9]

To confirm that the damage was cause because of the high amplitude of these harmonics, electrical field simulations and laboratory experiments were performed. This was confirmed by testing the cable and termination at fundamental frequency, followed by fundamental frequency superimposed with different high frequency signals . The simulations also showed that there was field concentration at the semiconductor layer as the stress grading layer used was not sufficient for the field at 12.4 kHz. As a solution, the cable terminations in the substation were changed from resistive graded to geometric terminations, which are not frequency dependant below the

MHz range [9]. Another case has also been used as example when a the 33kV oil-paper cable in London reporting high rates of failure. The purpose of this cable was to connect the AC grid to a rectifier supplying the London under ground Transport [10]. This example is interesting because initially it was never thought to be a case of failure due to high frequency harmonics. It was not until all other causes were eliminated, that the engineers finally arrived at this conclusion. Initially it was though that the faults were due to ionization. However, it was noticed that there was a common feature in these faults, which was a small pin-hole in the inner layers of the insulation. This is an interesting observation as this was previously observed during faults due to voltage surges of short duration. After eliminating reasons such as fault due to manufacturing and neutral instability, voltage surges and harmonics were investigated. However, after a detailed calculation of the voltage required to breakdown a deteriorated section of the cable and comparing it with the possible amplitude of the surge and taking into account the surge impedance of the transformers, this reason too was dismissed.

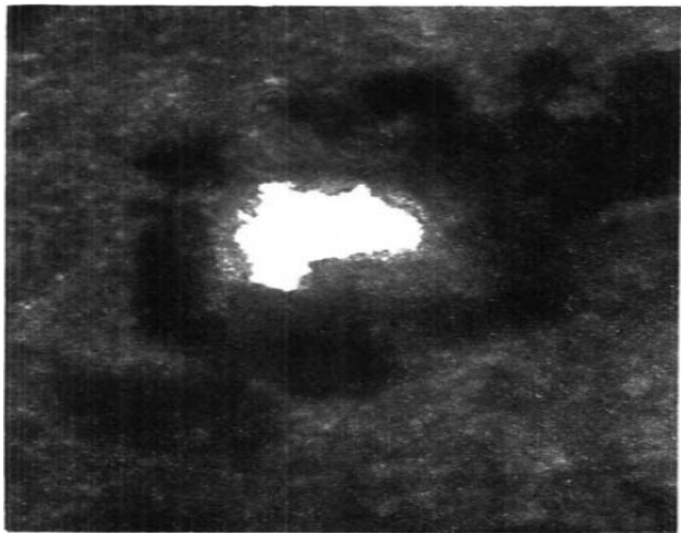

Figure 1.2: Pin-Hole in the insulation layer in the 33kV cable[11]

On observing the effect of the most dominant harmonics over a period of time, it was notices that the current wave forms showed existence of resonance conditions [11]. This led to establishing that harmonics were either causing deterioration of the insulation through

- increasing the number of internal discharges.
- increasing the dielectric losses

- increasing the crest of the operating voltage

With the passage of time the concerns regarding high frequency disturbances has grown. The shift towards a more decentralized grid and the adoption of more renewable energy sources, leads to an increased use of power electronic devices. The main source of the high frequency noises were the semiconductor devices like GTO thyristors and MOSFETs which were used in FACTS elements and Voltage source converters (VSC) [12]. Transmission systems using VSCs are increasingly installed as VSCs generate and absorb reactive power using power electronics switching. Power electronic components also enable working in HVDC, which is an advantage as it is better to use HVDC over long distances such as wind farms [13]. High frequency transients also occur very frequently is solid state transformers, due to their usage of semiconductor elements such as MOSFETs to change the input signal to a higher frequency [2]. While there is a continuous movement towards involving power electronics, there is simultaneously a need to understand how their involvement is going to affect the existing high voltage equipment to ensure smooth electricity distribution.

1.3. Methods used to generate High frequency

As the necessity to test high voltage insulation at high frequency is gaining recognition, more and more researchers are working on finding an ideal test set up and understanding the circuit requirements to conduct such a test. Through a literature survey, it was understood that most of these test are based on transformers and cable insulation, which are widely used and are under severe stress due to high frequency disturbances.

The test set up and the methods used to generate the high frequency signals depends mainly on the value of the test object and the frequency. For instance, some studies desire to know the time to breakdown of an insulation, only under one particular frequency and hence the frequency can remain fixed. Others aim to find the influence of only a few frequencies, superimposed on the fundamental frequency. For instance, the research in [2] investigates the effect of high frequency oscillations in the range of 5kHz to 15kHz, by superimposing on the power frequency to test transformer paper insulation. This study claims these disturbances to be nonstandard voltages, which arise mainly due to semiconductor devices used in combination with passive devices. To produce high frequencies signals, superimposed on the fundamental frequency, two sources are used, namely, a testing transformer which produces up to 40kV in series with a high frequency transformer, made with a nano crystalline core. The test was performed with only two cases, at 50Hz and at 50Hz combined with high frequency oscillations. The applied stress varied between 25 to 65kV/mm. The results were basically a comparison of the two cases. A similar attempt

to superimpose a high frequency waveform of 7kHz on a power frequency of 13 kVrms was made in [3] where the aim was to observe partial discharges and resistive heating in a XLPE cable terminations. This study provides a simulation-based analysis of high frequency testing at high voltage and realises the circuit by using a high-power amplifier and a high frequency transformer to produce the 7kHz signal. A similar situation is identified during the operation of a solid-state transformer (SST) which is mainly a combination of a transformer and power electronic devices that changes the signal to a higher frequency range before the transformer steps it up or down. According to [14], the conventional transformer in the SST uses an oil/paper insulation and the breakdown mechanism of such an insulation and the long-term effects of high frequency on it, is unknown so far. It is predicted that in the coming years, a SST will be more often used due to their added advantage of providing variable frequency. Hence, to test the insulation, here, they developed a half bridge out of SiC MOSFETs, as in fig. 1.3, which will produce the desired high frequency of 40kHz and 20kHz. Since the maximum amplitude that the signal can reach is only 5kV, a transformer is used to step it up to the desired test voltage.

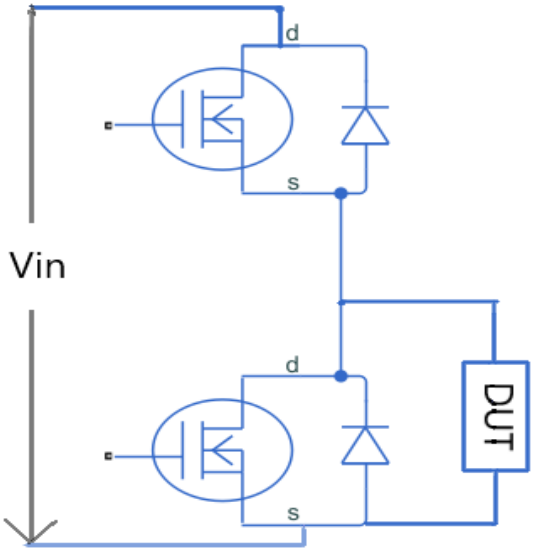

Figure 1.3: Pulsed High Frequency source

Probably the first-time air cored transformers were used with resonating RLC circuits can be found in Apparatus for transmission of electrical energy by Nikolai Tesla. From this concept arose the design of a tesla transformer which has previously been used in many studies to superimpose high frequency on high voltage fundamental frequencies. They have been also redesigned with a few modifications to suite the testing procedure as has been shown in [6, 7, 15].

The method used to generate the high voltage high frequency signal depends also, on the load capacitance, as mentioned before. When testing with DC, or at a low frequency, it is important to note that the impedance of the capacitance will be very high. This is not so when the frequency increases and with lower impedance, a higher demand for power arises [6]. Hence a capacitive load at high frequency, is placing a huge demand for power. With this in mind, we can discuss the common method for generating high voltage AC, which is a transformer. In [6], we see that these transformers have two main disadvantages; the requirement of a high-power voltage source and cost ineffective. This is because, when operating in high frequency, the iron core has to be replaced with a ferrite core. A ferrite core can take on much less magnetic flux density and so there is a need to reduce the number of turns. The requirement for a powerful voltage source is caused by the reactive power requirements of the capacitive load that has to pass the transformer and has to be full filled by the AC power source. Because of these disadvantages, it is strongly recommended to operate at resonance frequency, as in that case, the reactive power is not an issue. The voltage source now, need to supply only the active power. The secondary of the transformer resonates with the load capacitance and hence for a load of about 500 pF, at 15kHz, a 225 mH inductance is required. When this inductance has to be attained in a small transformer, the main issue that arises is that of a high self-capacitance. The proximity of the coils induces a large self-capacitance, which is, in many cases comparable to the load. As a result, the designed transformer self resonates in a frequency, much closer to the test frequency. There is also the problem of the ferrite core showing a flux non linearity, which leads to harmonics. The

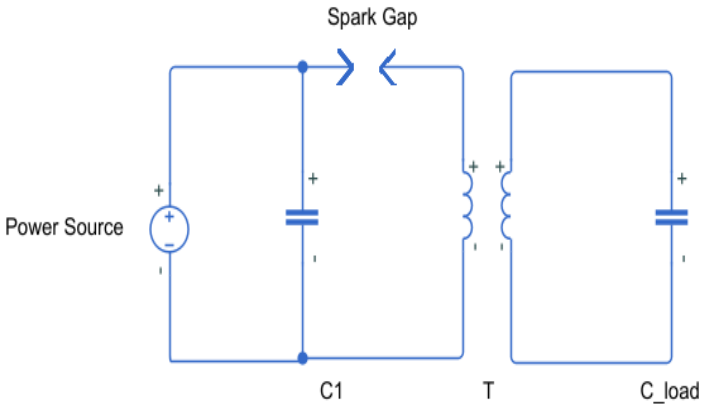

Figure 1.4: Tesla transformer T with sample C, 1. v. resonance capacitor C1,power supply (p. s.) and spark gap (s. g.)

use of a Tesla transformer as shown in fig. 1.4, is a means to avoid such problems as it uses coils couple via air and no core is present. This helps because the core is not present to introduce

any non-linearity and since the coils are larger and further apart, parasitic capacitance is reduced to a large extent. Another option for reducing the issue of parasitic capacitance, a more flexible option is to use a series resonance circuit, which is suggested in [16]. In this circuit, the value of parasitic capacitance and resistance can be limited by understanding the impact of coil geometry and adopting suitable winding practises, which will be discussed in Chapter 4. Such a circuit retains the advantage of being less demanding of power as the source only needs to supply the active power when operating at resonance. In the following chapter, this circuit is studied in detail and the elements needed to design it have been discussed.

1.4. Goals of research

The goal of this research is to investigate the effect that high frequency signals have on the high voltage insulation. Currently, only the 50Hz life time curve is used as reference for insulation aging,although, the need to test at higher frequencies also has been considered important in studies similar to this thesis. However, to reach our goal, we aim to produce similar life time curves for a range of frequencies. This will help in determining the contribution of an individual high frequency signal in insulation breakdown, or failure. To test insulation samples at high voltage and at high frequency, a specific set up needs to be designed such that the frequency can be varied. To a certain limit, a high-power amplifier can be used. This currently, could not be used for the entire range of frequencies as, the performance of amplifier is limited by the current and since the range of frequency being tested is wide, one amplifier cannot satisfy the entire process of testing. Therefore, the aim of the thesis is :

- To study the effect of high frequency signals on high voltage insulation material with the help of life time curves.

- For the testing, a thorough investigation needs to be done on the circuit requirements for testing.

These goals will be approached by answering the following research questions,

- What is the appropriate set up to test an insulation sample under high voltage and high frequency such that the frequency can be varied for each test?

- What are the calculations and criteria required to decide on an appropriate circuit for testing?

- What are the fundamental elements of the selected circuit and how do these elements influence its performance?

- How to precisely measure the above-mentioned elements and identify the sources of error.

- When an insulation is tested for breakdown using high power amplifier, how can we draw conclusions about the aging of insulation and its lifetime.

The following chapters will be an account of the experiments and studies done in order to find an answer to each of these questions. The answers and results obtained from these experiments will be analysed and certain conclusions can be drawn from them.

1.5. Thesis Layout

From the previous three sections, it s evident that our shift towards renewable energy and the increasing involvement of power electronic elements in our distribution system is unavoidable. It is well known that this move elevates a huge burden that we place on non renewable energy resources to satiate our energy demands. Hence the only reasonable way to move forwards is to understand how it will affect the equipment currently in use and be prepared for this transition. One of the main effects of this transition is going to be increase of high frequency signal. chapter 1 gives a summary of the background research done to understand the generation of these signals and precisely formulate the questions that this thesis will attempt to answer.

One of the main challenges of this thesis to design a high voltage high frequency source, so that the high frequency harmonics can be replicated for testing different kinds of insulation. Currently there are not many options available to test at high voltage when a vast range of frequency is to be covered. As high frequency harmonics are becoming more of a cause of failure, high frequency testing might be necessary in future. Chapter 2 mainly focuses on the analysis done on designing a high frequency source using series resonance

Chapter 3 sheds more light on the series resonance circuit and the suggestions on improving the performance of a high frequency inductor. The inductor hold great capabilities in improving the performance of a circuit and according to the test sample, it can be designed to reduce losses to a great extent.

Chapter 4 discusses the occurrence of self resonance and the impact of parasitic capacitance in the operation of a series resonance circuit. This chapter also gets into the details of what factor increase the parasitic capacitance of a coil and ways to measure the value as accurately as possible. Different methods include equations, through software and experimental methods.

Chapter 5 moves to testing insulation material through the use of an amplifier and function generator. A sample of oil paper insulation is tested under different frequencies for observing the time to breakdown.

Chapter 6 presents the observations from the experiments performed in chapter 5. The time to breakdown at different frequencies is analysed and presented in the form of various graphs.

Chapter 8 will summarize all the conclusions made from this thesis and formulate answers for the questions raised in chapter 1.

2

Series Resonance Circuit Design

For generating high frequency high voltage for testing insulation samples, IEC [16] recommends, two methods and advises to decide based on the test object. One method is to use a transformer and the other is to use a series resonance circuit. However, as discussed in chapter 1, using a transformer has complications such as non linearity through ferrite core, and a high value of parasitic capacitance.

Hence for this thesis, it was decided to investigate the design of a series resonance circuit. As the test object is capacitive, we aim to either design a variable inductor , such that we can reach resonance condition at the desired frequency, or add an element of variable capacitance to the test object.

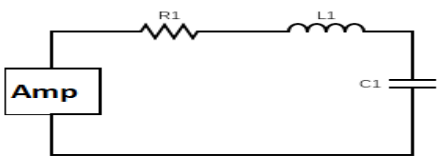

Figure 2.1: Schematic series resonance circuit

The idea is to use the circuit to test the insulation in the range of 50Hz to 15kHz with the maximum test voltage at 20kV. When operating in resonance, the reactance of the inductor cancels the reactance of the capacitor, and the power source has to only supply the active power, which will constitute of mostly

the resistive elements, combined together as R1 in Figure 2.1. Based on the above values, the required values of inductor and current were calculated using the equations:

$$L_1 = \frac{1}{C_1 \times \omega^2} \tag{2.1}$$

$$I = V \times (j \times \omega \times C_1) \tag{2.2}$$

Test object Capacitance	Freq = 15kHz	Freq = 5kHz
C_1 = 1 nF	L = 0.1126 H ; I = 1.884A	L = 1.01 H ; I = 0.628 A
C_1 = 5 nF	L = 0.0225 H ; I = 9.4A	L = 0.202 H ; I = 3.14 A

Table 2.1: Value of Inductance and current for 15 kHz and 5 kHz

From the calculations shown above it is evident that with the increase in load capacitance, our requirement for current to reach 20kV will be much higher. A current of around 9 Amperes is rather high, hence again creating an issue of selecting a powerful source. With the increase in current, the resistance of the circuit also needs to be taken into account, as with a higher resistance, and a higher current, the source would have supply more power to achieve the output voltage of 20kV. To test the performance of a series resonance circuit and verify if the calculations made in table 2.1 are correct, a coil of 13.5mH was made using solid Cu wire and ferrite core and capacitors of 10.2nF were used to form a series resonance circuit. According to the Equation 2.1, the circuit should resonate at 13.5 kHz. The circuit resonated at 12.1kHz, which basically shows the effect of the parasitic capacitance of the inductor as well as the error introduced through measuring equipment such as the probes and wires (discussed in chapter 4). The total resistance of the inductor measured through LCR meter was 8Ω. Due to this high resistance, the current through the inductor was also very low and hence, the voltage across the capacitor , which is meant to be our desired test voltage, is also very low. The current which passes through the inductor was 7.2 mA.

According to calculations, this should give a voltage across the capacitor of about just 8 volts. It can be concluded that increasing the capacitance is not a viable option as it is only going to increase the requirement for current, which will also lead to losses in other parts of the test set up, along with stress the power source. On searching online, our options for investing in an amplifier, which can provide the required test voltage at the necessary frequency were also extremely limited as not many of them catered to both, our range of frequency and our requirement for current.

The idea of using a transformer was also considered as it would be beneficial in reducing the stress

on the power source while providing a higher current to the load capacitance. It is also been used in many applications involving switch-mode power supplies and it's implementation and benefits are explained in [15, 17]. In the previous case where we use only an inductor, when the high current due to a large capacitance is an issue, using a high frequency transformer can be considered. The Figure 2.2 is a depiction of a high frequency transformer model with a turns ration n1:n2 . Here,

- R1 , L1 and C1 are the primary side winding resistance, leakage inductance and winding capacitance.
- R2, L2 and C2 are the secondary side winding resistance, leakage inductance and winding capacitance.
- C3 depicts the capacitance between the primary and secondary side
- Lm is the magnetising inductance
- Rf is the resistance due to the core

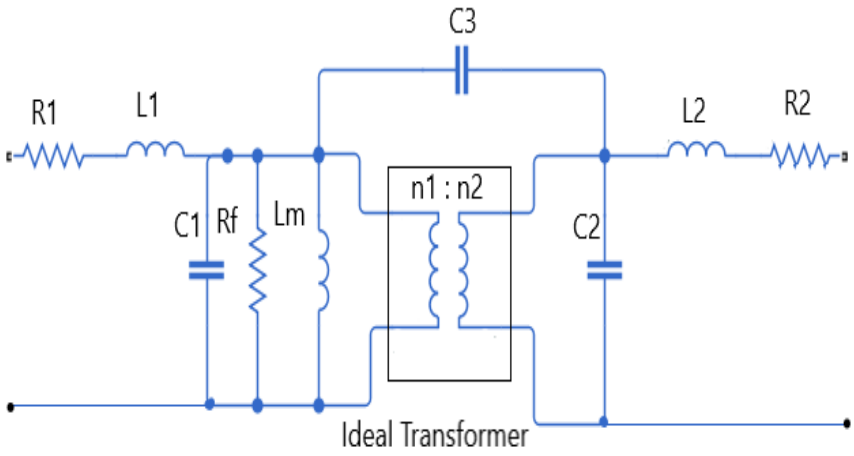

Figure 2.2: High frequency Transformer

Many of these parameters depend greatly on the geometry of the coil as will also be discussed in the upcoming chapters of this thesis. However, certain discussions in [17] and using circuit equation, we can decide if a high frequency transformer will serve the purpose. Taking up the example of using a 5nF load capacitance, we understand that the current required will be

9.4A at 15kHz to test at 20kV. It is suggested in [17] that we can use the leakage inductance of the transformer to form a resonance circuit with the stray capacitance elements. This is mainly said to be helpful in avoiding the voltage spikes, which occur in cases when the transformer is operated with non-resonant sources, such as PWM. However, this idea seemed worth investigating for our high frequency application as well. To obtain a high current in the secondary side, while not going for a high power source, we want the primary side to have more turns compared to the secondary, based on the transformer equation. This would mean a higher resistance on the primary side, as well. Referring to the fig. 2.3, we see the high frequency transformer circuit with all the elements referred to primary side. From the fig. 2.3, another problem due to the

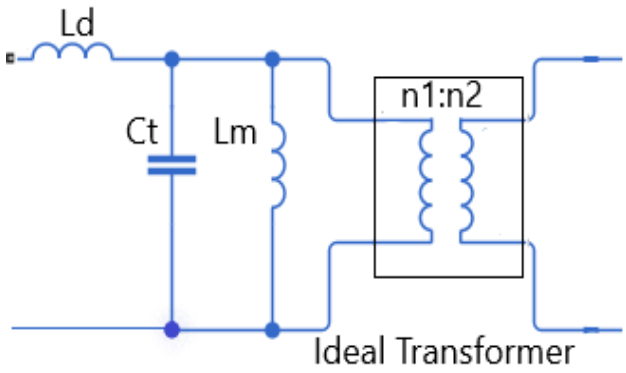

Figure 2.3: High frequency Transformer with elements referred to primary side

parasitic capacitance from the winding is visible. When referred to the primary side,the parasitic capacitance will be referred with the square of the turns ratio, which will lead to a large value of capacitance. To avoid this, the primary and secondary turns need to be kept very far apart. These are again the same issues that we face while designing a high frequency inductor, that arise mainly due to parasitic capacitance. In the following chapters, we try to look at various ways and means to measure this value accurately. Why this value poses to be so important, is because, when we want to test a single sample of insulation, it is actually less than 1nF. This comes very close to the value of parasitic capacitance that we estimate we have, from the coil. Added to this, there is the capacitance introduced through measuring equipment. If we are able to measure and essentially control the value of this capacitance, it will be easy to design a series resonance circuit and testing samples with lower current requirement and losses.

3

Inductor Design

Chapter 2 introduces the concept of a series resonance circuit and explains the role it can play in high voltage and high frequency testing. In this chapter, we look at the criteria to design an inductor for the series resonance circuit and understand how the inductor design influences its working.

3.1. Inductance

The inductance of any coil depends on the wire geometry, number of turns, the permeability of the core (μ), and winding geometry. The winding of an inductor not just decides the value of inductance but also determines the losses in the inductor and hence the overall performance of the circuit.

Once we know the value of the inductance we require and the maximum current passing through it, we are able to work out the other parameters based on a few criterion, well defined in [18] and [19]. The following criteria are suggested :

- Firstly, based on the maximum current, the maximum core flux density can be evaluated, so that we do not operate at the saturation flux density. From the known equation of a

magnetic circuit, $N \times I = B \times A_c \times R_g$ we can write $N \times I_{max} = B_{max} \times \frac{l_g}{\mu_o}$. Here,

  - N: Number of turns
  - I and I_{max} the current and the maximum current
  - B_{max} is the maximum flux density
  - l_g is the air gap length

- Next, we try to attain the value of our specific inductance , L, through $L = \frac{\mu_o \times A_c \times n^2}{l_g}$; where A_c is the cross sectional area of the core.

- The core shape and the winding area must also be considered. Different core shapes and core material are suitable for different purpose. These details are discussed in the following sections.

- Finally, the resistance of the winding, is determined by $\rho \times \frac{N \times MLT}{A_w}$ where MLT is the mean-length-per-turn, of basically the length of the wire for one turn.

The criteria mentioned are mainly guidelines to design the inductor. The value of different parameters can be selected based on the purpose that the inductor will satisfy. For example, for high frequency, a ferrite or a nano crystalline core is preferred. Different shapes such as torroid, E shaped, U shaped are meant for different purposes and can be found in ferrite core suppliers website very easily. A core with high permeability, results basically, in a compact inductor with fewer turns.
The core material of an inductor is chosen based on frequency, saturation flux, current ripple. One of the main challenges is that there are numerous aspects that effect the performance of an inductor. In our case, where we are concerned with operating the inductor at high frequency, the size of the passive components do come down, however, the losses increase and this leads to a drop in efficiency. While selecting the core, the aim is to find a balance between system efficiency, power density and cost [20].
Some of the materials used for inductor designs are :

1. Ferrite: They are one of the most commonly used material for high frequency operation

because they provide low losses at very high frequency. They are chemically inert ceramics, which have high resistivity an low saturation induction. The Mn-Zn ferrite material is used to operate up to a several kHz and have a high permeability. The Ni-Zn ferrite is used for even higher frequencies, in the MHz range and has a high resistivity.

2. Powdered Iron Core: This material is used mainly because of the distributed air gap present within this material and the possibility of varying the permeability by mixing different quantities of iron or metal alloy. They however, have a lower permeability and higher saturation flux compared to Ferrites. The distributed air gap and low permeability contributes in bringing down the resistance and core losses by a large extent[21].

3. Nano-crystalline: These are materials with the combined advantage of high frequency operation from Silicon and the high flux saturation as in Fe-Si. A Core made of nano-crystalline material are a good choice provided cost is not an issue.

These materials were tested for the amount of loss generated in [22] under sine wave and triangular wave. It was found that the maximum losses occur in Fe-Si(nano-crystalline) or amorphous cores. Powdered cores are comparatively better, where as ferrite core generate the least amount of losses. The shape of the core that we choose is also influential on the performance of out inductor.Toroid core hold an advantage of being cheap and in a single piece. This shape for a core also efficiently keeps the electromagnetic interference low, as it forcibly constraints the magnetic flux as the field lines form a closed circular loop [22]. Winding turns in a toroid core is however, complex as it is more difficult than winding on a core with a bobbin, hence might prove expensive [23]. It is even difficult to have an air gap in the toroid core. Here, shapes such as UU and E cores provide a viable solution. UU cores also provide better window utilization and when used with curved corners, uneven magnetic field concentration can be taken care of. The EE shaped cores go a step further and provide gaping only in the central leg which reduced electromagnetic interference as well as fringing flux. The U type and EE type are also better at cooling as well, as compared to toroid core. They are however, not very useful when it comes to high frequency operations as the interference is still very high. A pot core fits this situation better [24].

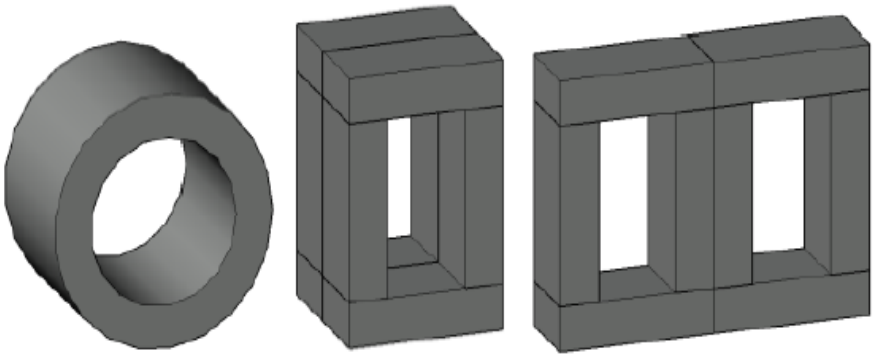

Figure 3.1: 3D depiction of transformer cores: Toroid, UU,EE [24]

One phenomena, which should be carefully dealt with, specially in the case of designing high frequency inductors is the phenomena of fringing flux.This phenomena occurs when the flux flowing in a magnetic core spread out in the presence of a different medium, such as an air gap. Fringing flux causes a number of problems which essentially deteriorated the performance of the inductor [25]. When operating in high frequency, it increases the length of the magnetic flux path of the inductor hence bringing down the reluctance. This induces an error in the inductance value aimed to be achieved by the designer. Depending on the air gap the flux fringes more severely and strikes the core, inducing eddy current, and when it strikes the copper, induces heating. Fringing flux also tends to lead to premature saturation of the core [20].

3.2. Lumped Parameter representation of Inductor

When depicting an inductor, or modelling them in programs such as SIMULINK, it is easier to depict inductor using lumped parameters. A Lumped parameter model helps with mathematical calculations but when working with high frequencies, it induces a certain amount of error which can be missed to account for. We know that as the frequency rises, so does the ac resistance of the coil, specially if made with solid wire. Frequency rise also attributes to concerns regarding self-resonance and self-capacitance of a coil. Operating an inductor at a high frequency means consciously avoiding operation close to it's resonance frequency. The stray or parasitic capacitance occurs in the winding itself, between the turn, between two layers or between the winding and the core. Resistive losses occur through winding resistance and core resistance [21].

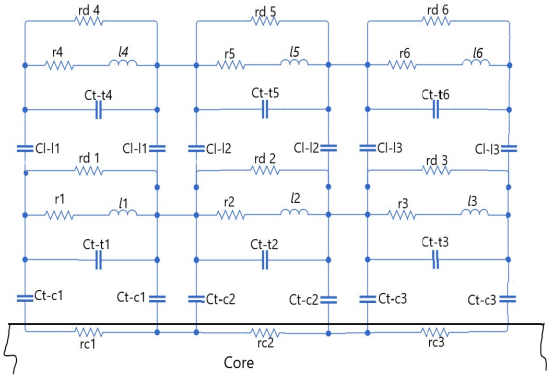

Figure 3.2: Detailed Model of two layer inductor

In Figure 3.2, c_{t-tj} is the turn-to-turn capacitance of each j-th turn, c_{t-cj} is the turn-to-core capacitance and c_{l-l} is the layer-to-layer capacitance. Parasitic resistances are the winding resistance r_j the core resistance r_{c-j} associated with the finite resistivity of the inductor core, and the resistance of the dielectric material coated on the wire r_{dj}. To reduce the complexity of the circuit and make it easier for calculation, the circuit shown in Figure 3.2 is modified into a lumped parameter equivalent circuit such as Figure 3.3. Here , R is a combination of winding and core resistance and is frequency dependant.

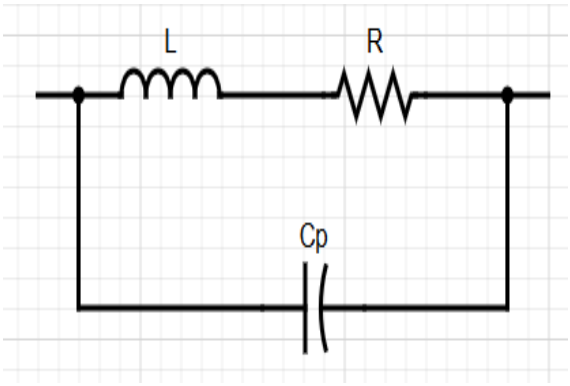

Figure 3.3: Lumped parameter equivalent circuit

In [26], Figure 3.4 is used to depict power loss of the core with R_p and total resistance of the winding with R_s, which is an alternate used to model the inductor.

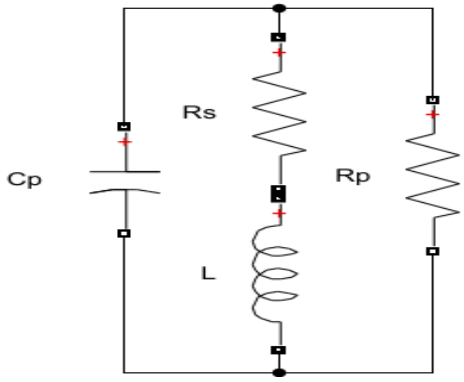

Figure 3.4: Lumped parameter model with core and winding losses

3.2.1. Parasitic Capacitance

Parasitic capacitance is a hindrance to the inductor being operated in high frequency. Considering the parasitic capacitance is important, as this will determine the self resonant frequency of the coil. Hence we want to keep the parasitic capacitance as low as possible so that the self resonant frequency of the inductor is much higher in comparison to the frequency of operation. The parasitic capacitance is in parallel with the inductor and hence, beyond the self resonant frequency, similar to the effect in any parallel resonance circuit, the inductor starts behaving like a capacitor. Parasitic capacitance from due to the geometry of the coil and occurs in the following areas:

- Turn-to-turn
- Turn-to-shield
- Layer-to-layer
- Layer-to-core

The remaining parts of this section is going to present a summary from a few studies and research papers, which have experimented with coils and their parasitic capacitance. These studies have successfully been able to conclude on a few factors that influence these values. For an air cored single layer coil, the parasitic capacitance is mainly influenced by the geometry of the winding and the wire itself. [27] studies a similar coil for operating in high frequency (in the range of a few hundred kHz). Only the turn-to-turn and turn-to-shield capacitance is considered in this paper and the following points are concluded:

- If the distance between turns (pitch) increases, turn-to-turn capacitance decreases.
- If the diameter of turn (D) increases, turn-to-turn capacitance increases.
- If the radius of the wire used increases,the turn-to-turn capacitance increases.
- If the distance from the shield is increased, Turn-to -shield capacitance decreases.
- If the number of turns in the coil increase, the turn-to-turn capacitance increases.(Assuming capacitance between all adjacent turns are equal i.e C_t,)

$$C = \frac{C_t}{n-1} \tag{3.1}$$

Based on the above parameters, in [28], an equation is derived to obtain the self capacitance of an inductor. This equation is only based on the coil's geometrical parameters and the number of layers it contains. The derivation is used in this thesis to calculate the parasitic capacitance and is discussed in detail in chapter 4. The total stray capacitance of inductors consists of the following components:

- The turn-to-turn capacitance between turns of the same layer
- The turn-to-turn capacitance between turns of adjacent layers
- the turn-to-core and turn-to-shield capacitance

The study also reports the influence of the wire insulation of the parasitic capacitance as:

- In cases where the thickness of the insulation of the wire is considerable to the wire's diameter: higher the permitivity of the insulation material, higher will be the stray capacitance.
- If thickness of the insulation itself increases, the parasitic capacitance decreases.

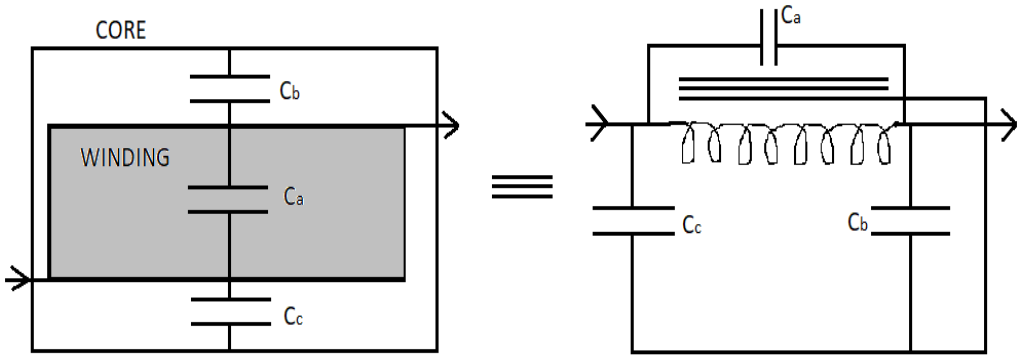

Figure 3.5: Depiction of different parasitic capacitance

Besides the coil geometry, it is also important to understand the influence of a core in the parasitic capacitance value. According to [19],the following observations have been made, with reference to fig. 3.5

- If the core is not connected to either end of the winding, the parasitic capacitance is observed to be the lowest.

- If one end of the winding is connected to the core, it short-circuits one of the end capacitance, which then makes the other end capacitance directly in parallel to C_a.

- Although cores are not made out of reactive materials, such as ferrite, which are generally inert, it is recommended to seal the circuit in an airtight manner, as moisture tends to increase the parasitic capacitance.

Besides using a core, another option to increase the inductance is using a multilayered coil. With this arise new sources of parasitic capacitance.It has been proved mathematically as well as experimentally that, if number of layers increases, the stray capacitance decreases. This is because the capacitance between each layer is added in series. However, when operating in higher frequencies, the resistance of the coil will also increase. Hence it is not a prudent solution to keep increasing layers to bring down the parasitic capacitance. This is also verified in [23], where, it is given that among all multi layer inductors, the capacitance in two layered coils is the global maximum.

When the number of layers in an inductor are high, [19] introduces a parameter

$$C_a = \frac{4C_l(p-1)}{3p^{(2)}}; \tag{3.2}$$

which is the hypothetical capacitance across the winding as seen in fig. 3.5. Here, C_l is the capacitance between adjacent layers an p is the number of layers. The parasitic capacitance is categorised as:

- C_c, the direct capacitance between the core and the first layer.

- C_b, the direct capacitance between the core and the topmost surface of the winding.

Parasitic capacitance in multi layer coils is also discussed more deeply in [26]. This research provides the equation for stray capacitance as a combination of layer-to-layer capacitance and layer to core. We already know the parameters in a coil which influence the stray capacitance. From [26], we get an idea of which are the more dominant parameters in certain cases.

- If inductor has multiple layers, layer-to-layer capacitance is dominant compared to layer to core.

- If surface area of the capacitive plate increases, layer-to-layer capacitance increases.(Layer of the winding are treated as capacitive plates)

- If diameter of a single strand increases or if number of strands in the wire increases, the layer-to-layer capacitance decreases (This paper studies coils made only out of Litz wires, hence number of strands).

With the increase in operating frequency, the parasitic capacitance also increases. Through experimental verification, [21] suggests that when operating within 20% of the self resonant frequency, the inductor can be modelled with just a resistance for loss component and parasitic capacitance can be neglected.

A high frequency inductor is used for various applications.For instance, we use the inductor in a series resonance circuit and we require a high inductance with a low parasitic capacitance. Similar coils are also used in chokes and converter circuits. The authors of [23] investigate the stray capacitance in common and differential mode of chokes, but initially delves into single layer solenoid and losses in terms of the methods of winding. The coils are wound on a toroid core as they provide higher permeability compared to other core shapes. The winding patterns of two layered coil in a toroid core is shown in

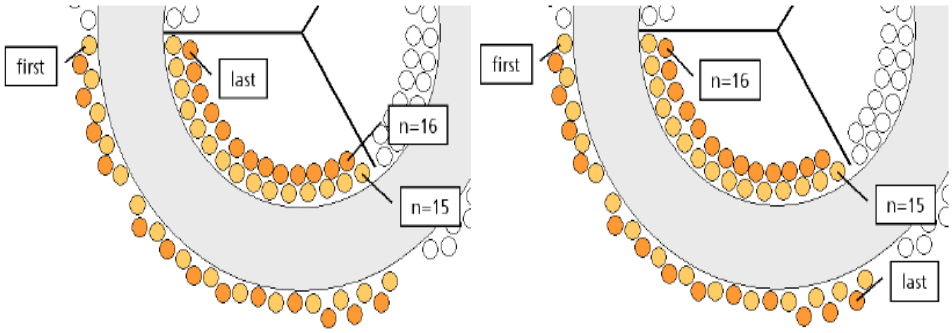

Figure 3.6: The ongoing wound second layer on the left and the equally directed on the right [23]

The maximum capacitance has the two layered winding with the beginning and the end of the winding in close proximity. If second layer winding is wound in the inverse direction as the first , the capacitance is 133% the capacitance of the winding ,if wound in the same direction.

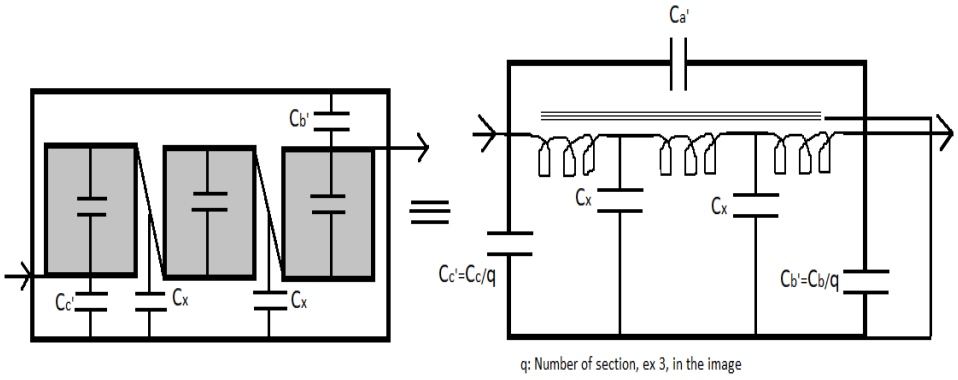

Figure 3.7: Self capacitance in three section winding [19]

To effectively reduce the parasitic capacitance, the entire coil can be divided into sections and wound side by side as shown in Figure 3.7. Sectioning reduces the capacitance in two ways. Firstly, C_l is is divided by the number of sections, q. Secondly, the number of layers, p, is multiplied by q. Thus in Equation 3.2 , C_a gets divided by q^2 . Is series resonance circuit, the parasitic capacitance, which is in shunt with the inductor, the losses mainly occur because of the circulating current in this loop. The authors of [19] has also established a relation between the geometry and parasitic capacitance:

$$C_s \alpha \frac{(b)(l)}{h} \tag{3.3}$$

Where,

b = width of the winding

l = mean turn length

h = Height of the winding

It is an advantage to use a winding area which is tall in comparison with its breadth. Sectionalizing is an artificial method of achieving this if the given winding area is unfavourable. The benefits of a single layer winding, which is also recommended for high frequency operations in [21, 26] are discussed. The self capacitance reflected across the terminals of a winding having N turns, due to the capacitance between a pair of adjacent turns, is $(1/N)$ x (the adjacent-turn capacitance).So, the total contribution of the adjacent turn capacitance is only significant when there are few turns.Only in a single layer winding does this becomes important. In a single layer winding, this is the only capacitance that needs to be calculated, provided a core is not used. A single layer winding also keeps the ac resistance low which is beneficial for operating at high frequency.

3.2.2. Resistive losses

As discussed before, resistance in a coil increases due to high frequency. The dc resistance of a coil is predominantly due to the resistance of the wire used. This depends on the resistivity , cross sectional area and length of the wire. When stranded wires are used, we take the effective area of cross section. When operating in high frequency, if we observe a high ac resistance, it is preferable to switch to a coil made out of Litz wire. This can start occurring from a few tens of kHz on wards. Litz wire are basically bundled wires, that is, many strands of wires twisted together, which means each strand has a very small cross sectional area. This helps in reducing the resistance due to skin and proximity effect [26]. A few other points which can help in reducing the ac resistance are discussed in [21]

- Resistive core loss is reduced drastically when introducing distributed air gaps and using low permeability, like iron core.
- If number of layers increase, ac resistance increases.
- If flux density is high, core losses are much more predominant that copper losses.

In general, the ac resistance of a coil can be found using the quality factor, as done in [21] or by deriving an equation specific to each coil, some examples given in [26, 29]. As explained in [26] , if the diameter of a single strand in the Liz wire used is lesser than the skin depth, the AC and DC resistance turn out to be equal.

4

Parasitic capacitance and its Measurement

In the previous chapter, the main focus was on designing an inductor and understanding the representation of lumped parameters model. these parameters were also discussed in chapter 3. This chapter will focus on the parasitic capacitance of a coil and the influence it has on the inductors operation.

4.1. Methods of verifying capacitance

As mentioned in chapter 3, there has been a variety of research done on arriving at a accurate method of calculating the parasitic capacitance of a coil. This section contains the explanation of how three methods were employed in calculating the stray capacitance of one coil and verifying it against each other to understand their short comings. The first method is to calculate the capacitance using empirically derived formulas and modifying them for a single layered air core coil with reference to [19, 27, 28]. The second method used is through the help of COMSOL-multi physics, where a model of the coil is created and the capacitance is calculated using it's total energy or with the aid of the mutual capacitance. The third method is to wind the coil as close to the specification as possible and test it to get the self resonance frequency , from which the

parasitic capacitance can be calculated.

4.1.1. Through calculation from equations:

As discussed previously, a coil has different sources of stray capacitance , based on its geometry , orientation and its functions. A single layer air core coil, has the main source of parasitic capacitance, as the ones present between each turn. Since capacitance is an inverse function of distance, the capacitance present between non adjacent turns can conveniently be neglected. The above assumption is applied in most derived equations for calculating stray capacitance. In [28] and [30], the turn to turn capacitance is studied in detail by considering only the geometry of the two turns involved. Hence to make these calculations the following parameters are required:

- Inner diameter of wire
- Outer diameter of wire
- length of a turn (2π x radius of the turn)
- Dielectric constant of the insulation material (ϵ_r)

To get these parameters, a single layer air core coil was wound and the physical dimensions were taken using vernier calipers. To calculate the dielectric constant of the insulation the following procedure was used: A piece of the wire used for the coil is taken (20cm, in this case). using an equally long aluminium tape, the outside of the insulation coating is wrapped making sure no air bubbles or gaps are trapped. The outer and inner diameter if the wire is taken and the capacitance of the wire is measured using an LCR meters, between the wire conductor and the Al tape. The values are then substituted in the equation below

$$C = \frac{2\pi\epsilon_0\epsilon_r L}{ln\frac{b}{a}} \tag{4.1}$$

For the coil under consideration, the values were :

wire Dimensions	
Outer Diameter (2b)	3.5mm
Inner Diameter (2a)	1.8mm
Length (L)	20cm
Capacitance	71.08 pF

Table 4.1: Dimensions of wire to measure dielectric constant

Based on these values, the dielectric constant of insulation material(ϵ_r) comes out as approximately 4.3.

Now since all the parameters are available to us, the equation given in [30] and [28] can be used. The theory used in this paper is to divide the capacitance between any two turn into the series combination of the capacitance of:

- The insulation coating of first turn
- The air gap between the two turns
- The insulation coating between two turns

These three sections of the entire parasitic capacitance is shown in Figure 4.1.

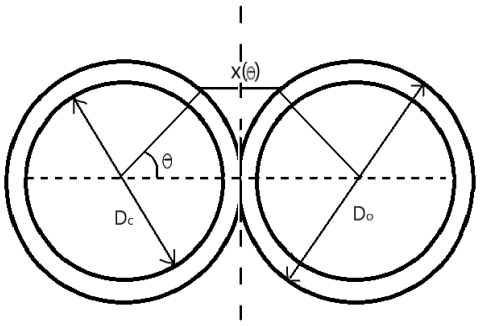

Figure 4.1: Adjacent turns with Electric field path, x

Figure 4.1 shows the placement of any two adjacent turns, in the same layer or even in different layers. This applies for all the turns in a coil which are not immediately next to the core or the outer periphery, and hence have similar turns on all sides. Next, an equation for elementary capacitance (dC) between two opposite surfaces(dS) is given as :

$$dC = \epsilon \frac{dS}{x} \tag{4.2}$$

where x is the length of the line of electric field connecting the two surfaces. To accommodate for the location of the winding, 'x' is kept a a variable which can be related to the angular co-ordinate θ. Since the conductors are assumed to be surrounded on all sides with similar conductors, the electric field lines coming from one conductor will reach all its immediate neighbours. Hence to decide the range of θ, we can say from Figure 4.2, that each turn shares a perimeter of $\frac{\pi}{3}$ with the neighbouring turn. Hence , the dC obtained fromEquation 4.2 will be integrated over $\frac{\pi}{3}$.

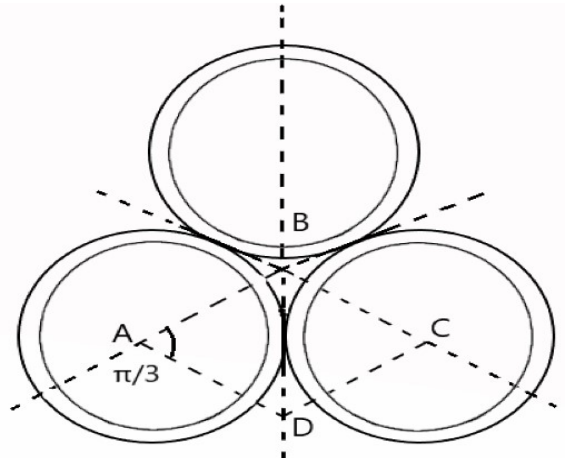

Figure 4.2: Single cell depiction for multi-layer winding

Integration of this equivalent capacitance over the basic cell, will result in the turn to turn capacitance that we require. For this purpose, first, the value of θ is defined, as θ^* , which is the point where the elementary capacitance of the air gap will be equal to the series capacitance of the insulation coating. With these boundaries established, we assume that the thickness of the insulation coating is small enough to use the equation for parallel plate capacitance. In that situation the equation we arrive at is;

$$C_1 = \frac{\epsilon_0 \epsilon_r \theta^* D_a L_t}{s} \tag{4.3}$$

where, s is the insulation thickness and L_t is the turn length and D_a is the average diameter of the insulation. From Figure 4.1 we see that for the value of θ which is less than θ^*, the air gap capacitance will be larger than the capacitance of the insulation. Since all 3 capacitance are in series, for these values of θ, we will only consider the capacitance of the two insulation coatings.

$$C_i = \frac{C_1}{2} = \frac{\epsilon_0 \epsilon_r \theta^* D_a L_t}{s} \tag{4.4}$$

For $\theta^* < | \theta | \leq \frac{\pi}{6}$, the capacitance of the air gap in more predominant when considered in series. We define the path $x(\theta) = D_o(1 - cos(\theta))$, as can be seen from Figure 4.1.Now it is possible to obtain the elementary air gap capacitance from the Equation 4.2 by substitution:

$$dC_g = \epsilon \frac{l_t \times D_o}{2(\theta)} d\theta \tag{4.5}$$

Simplifying and integrating it in the range where we find the air gap capacitance to be more dominant we get:

$$C_a = \epsilon_0 L_t [cot(\frac{\theta^*}{2}) - 3.732] \tag{4.6}$$

Hence the total capacitance becomes:

$$C_t = C_i + C_a = \epsilon_0 L_t [\frac{\epsilon_r \theta^* D_a}{2s} + cot(\frac{\theta^*}{2}) - 3.732] \tag{4.7}$$

Where,

$$\theta^* = arccos(1 - \frac{2s}{\epsilon_r D_a}) \tag{4.8}$$

The θ^* of the coil with dimensions as given in Table 4.1 is 0.55 radians. With this value, the turn-to-turn capacitance(C_t) is calculated as 9.9212 pF.

$$C_s = 1.618 C_t \tag{4.9}$$

Therefore total capacitance is 17.05 pF.

4.1.2. Through COMSOL-Multiphysics:

A number of methods exist in COMSOL to arrive at the capacitance between conductors. They vary mainly based on ease of calculation and the kind of geometry that needs to be analysed.

One of the methods is to generate a capacitance matrix, which is available as a function in COMSOL itself. In a typical electrical system, which would natural contain more than one conductor, it is not possible to constrain ourselves to just a single source of stray capacitance. As discussed before, analysis of parasitic capacitance, through various methods relies, mainly on the assumptions that the author forms. When it comes to stray capacitance in a coil, based on the geometry and the orientation , we can decide which source of parasitic capacitance will be most predominant and then move ahead with that. Considering the case where the number of conductors is n. This can be done by studying the geometry under parametric sweep, which enables one terminal to be excited at a time. When we assign our terminals as different conductors, we get a matrix which is obtained by exciting each conductor individually and calculating the capacitance between that conductor and the other non-excited terminals. As a result, we can obtain different matrices such as Maxwell's capacitance, Inverse capacitance, Mutual capacitance.

Mutual Capacitance: For an n conductor system, it is convenient to arrange the mutual capacitance in a matrix such as:

$$\begin{bmatrix} C_{m11} & C_{m12} & \dots & C_{m1n} \\ C_{m21} & \dots & & C_{m2n} \\ . & & . & \\ . & & & . \\ C_{mn1} & C_{mn2} & \dots & C_{mnn} \end{bmatrix}$$

The coefficients of this matrix are called lumped capacitance, which are basically how we represent capacitance in our inductor diagram representing all elements as lumped parameters.
Maxwell's Capacitance: Another commonly used form of capacitance matrix is the Maxwell's capacitance matrix.The Maxwell capacitance matrix describes a relation between the charge of the i^{th} conductor to the voltages of all conductors in the system. The Maxwell's capacitance and the mutual capacitance matrices are interchangeable. This can be done in COMSOL and the mathematical concept behind it is explained through equations in Appendix A taken from [31] .

Another method used is to assign the appropriate voltage drop to each conductor and then compute the electrical energy density of the coil. This method is mainly the application of $W = \frac{1}{2}CV^2$. For instance, if there are 4 turns in a coil, the voltage to the top most conductor is 1V and the following conductors receive, 0.66V, 0.33V and 0V subsequently. This can similarly be done for any number of turns. The materials are assigned their properties as desired and the

model is studies under the stationary study. In this particular simulation, the surrounding is given as air, the insulation permitivity as calculated from Equation 4.1, and copper conductors. This gives us an option to compute the surface integral of the electrical energy density in the entire area which excludes the conductor. The result obtained from this simulation gave a capacitance of 21.784 pF.

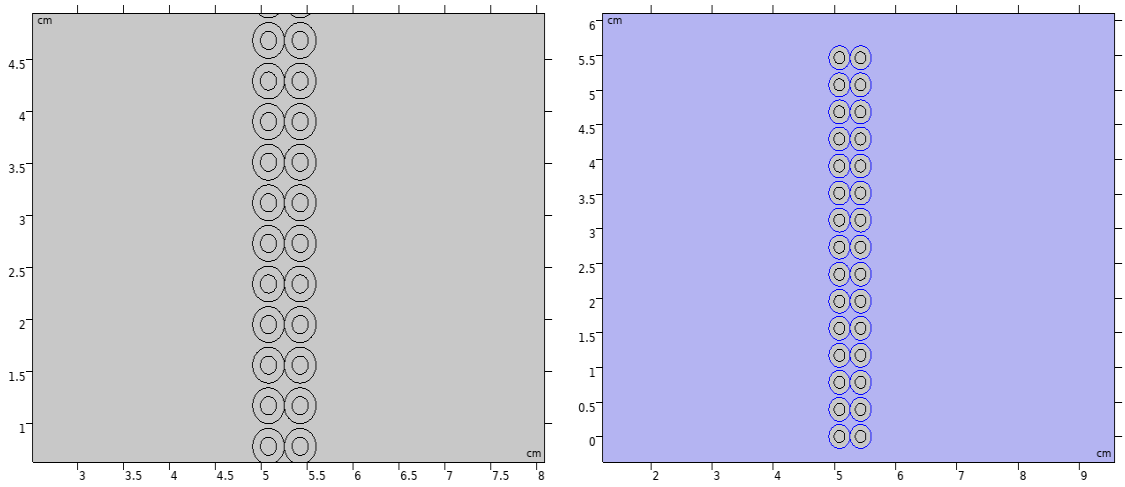

(a) Conductors arranged for 2 layer coil, 30 Turns (b) Surface Integral

Figure 4.3: Conductors and area studied for electric energy density

4.1.3. Through Experimental measurement:

The parasitic capacitance, when measured practically is done through the help of a function generator and an oscilloscope, as depicted in Figure 4.4.

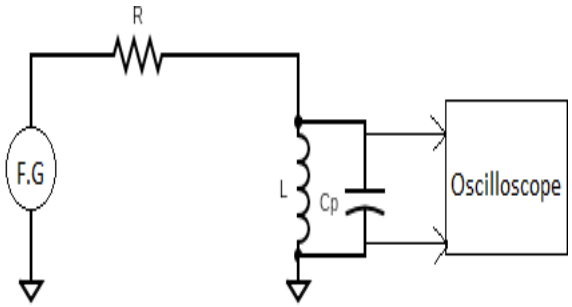

Figure 4.4: Experimental measurements

From the function generator, a square wave is produced which , on every rise and fall produces an LC oscillation which is damped by the resistance. From this oscillation, the time period is noted and with the inductance value of the coil, the parasitic capacitance value is calculated, based on

$$\omega = \frac{1}{\sqrt{L}C_p} \tag{4.10}$$

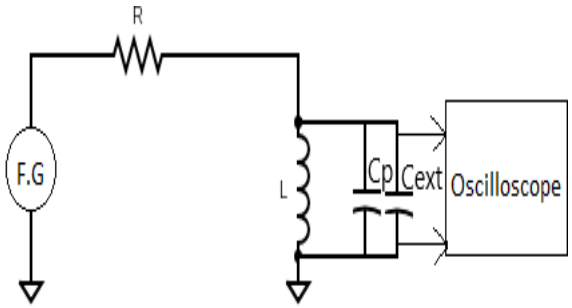

Figure 4.5: Experimental measurements with external capacitance

It is observed that the value of capacitance measured experimentally is not very reliable as it fluctuates with even a slight change in any parameter. This has many reasons.

- Resolution of the oscilloscope screen: Since we attempt to read the time period directly from the oscilloscope, the resolution of the screen can be a source of error. This is simply because of the error due to observation as we might not be able to detect the peaks very clearly. During the initial measurement trough oscilloscope , this kind of error crept in very frequently. From 4.10, we see that parasitic capacitance will be inversely related to the square of the frequency. Hence even a slight variation in reading the time period modified the capacitance to a large extent.

- The accuracy of the oscilloscope: The result of the experiment also depend on how well the oscilloscope samples the output.

- Another reason for errors is the inbuilt impedance in the probes and the input resistance and capacitance of the oscilloscope. Even the connectors, such as BnC connectors induce a few pF of capacitance(between 2-5 pF). The parasitic capacitance that we measure ,is sometimes comparable to the value of the internal impedance of the devices that we use for measurement, which is makes the two values indistinguishable.

- The components used, such as the external capacitance (as shown in fig. 4.5 and resistance are not always properly connected.

- When calculating using the equations in section 4.1.1, we assumed the inductance, capacitance and resistance to be lumped parameters, which is an approach created for mathematical convenience[32].

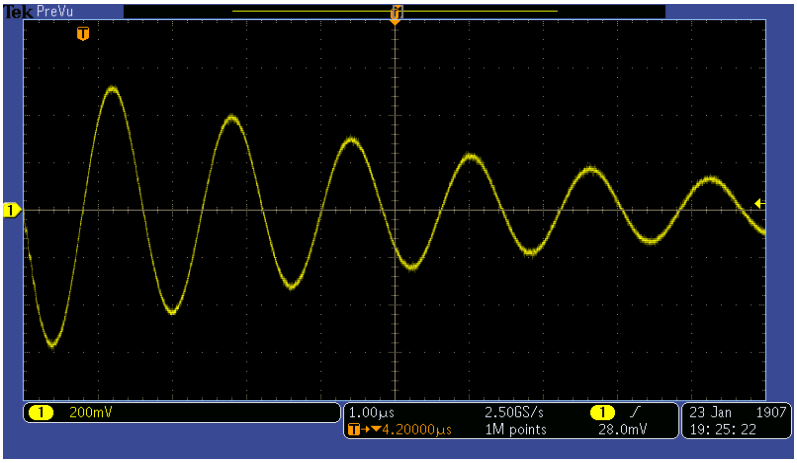

Figure 4.6: LC oscillation observed in oscilloscope

Since it is now known that various external elements tamper with the measurement of parasitic capacitance, it is important to know the origin of these error causing elements and understand methods to reduce their effect.

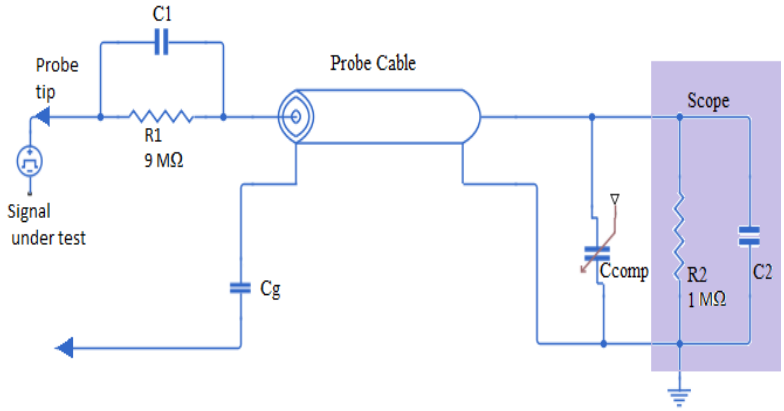

Figure 4.7: Measurement with a 10x Probe

When the oscilloscope is used with 1x and 10x probe, the results varies due to the internal construction of the probe. When the probe is set to 1x ratio, there is no attenuation and the voltage at the probe tip is measured directly. However, when using 10x probes, there is a resistor of 9MΩ at the probe, which , in combination with the 1MΩ resistor at the oscilloscope input resistance, creates a voltage divider. This also brings into play the capacitance (C1 from Figure 4.7), which is in series combination with Cg and C2. The combination of impedance of the circuit and input impedance of the oscilloscope and probe give rise to capacitive loading and resistive loading. When operating at high frequency, the capacitance involved in the probe and

oscilloscope become significant and affect the measurement. Measuring at high frequency also leads to a lot of disturbances while saving or recording a wave , hence reproducing or plotting it elsewhere, such as MATLAB, is difficult. Loading due to probes can be categorised as resistive and capacitive loading. When measuring, both types of loading do occur simultaneously, their influence on the measurement depending on how high the probe resistance and capacitance actually is. Another aspect to consider is also the inductance induced due to the ground wire used in the probe, which produces a ringing effect because of the interaction with the capacitance of the probe. The amount of this ringing is determined by the values of L and C in the probe [33].

Resistive Loading: Resistive loading , as the name suggests will be calculated entirely based on the resistances involved in the scope and the probe. Understanding from Figure 4.7, the circuit will become a voltage divider. Hence, the resistive loading only affects the amplitude of the signal [34].

Capacitive Loading: The capacitive loading is more dominant as the signal frequency increases. It mainly effects the rise and the fall time on the waveform, hence decreasing the amplitude of any high frequency details in the signal.

Verifying the capacitance due to probes and measurement equipment:

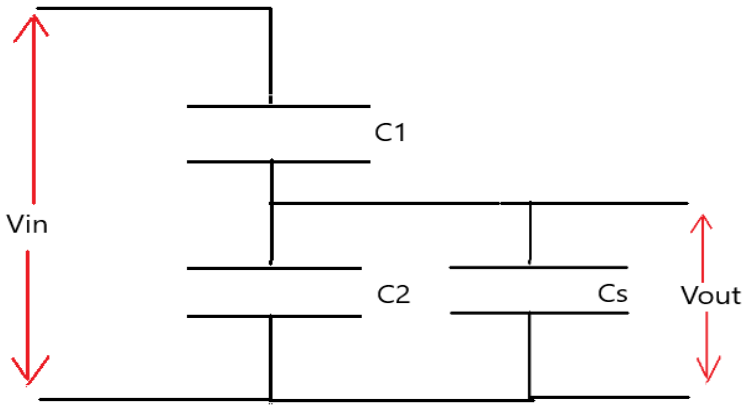

Figure 4.8: Capacitive Divider

The capacitance due to the probe was measured using a capacitive divider of known value as shown in Figure 4.8. A few different values of capacitance were selected for C_1 and C_2, and the voltage drop across one of them was measured using the same probe used for the parasitic capacitance measurement(Value of capacitors chosen: 10pF, 13pF, 559.2pF). The oscilloscope induces an impedance of around 1MΩ. Since the 1MΩ impedance will come in parallel with the

C_2 and C_s, an extremely large value of these two will make them insignificant in comparison and a voltage reading cannot be obtained. This is resolved by choosing the frequency carefully and for the capacitors selected, in the range of pF, any frequency above 1kHz was resulting in a constant output voltage. With these calculations,the value of C_s obtained were:

- At 10x : 11.44 pF
- At 1x :106.65 pF

The above values were also cross verified by using LCR meter, which gave a capacitance of about 15.42 pF. When measuring using 1X setting, the capacitance comes up to 107.71 pF. With the two previous methods of measurement, i.e., with COMSOL-Multi-physics and the equations, we know that the capacitance is in the range of 15-20 pF. Hence the probe capacitance at 1X is almost an entire order higher than this, making this method inaccurate. Using 10X setting to measure is also considered more accurate , as it reduces source loading [34, 35].
To further assure that the difference in the experimental values arose only due to the induced values from the measuring instruments, the same capacitive divider was measured using a better probe which had a capacitance of only 4pF. While the output voltage read before was incorrect by 36% , the value measured now was off only by 12%.

The values obtained from this experiment are given in the table below:

Value	No C_a	C_a =814.3pF	C_a=1637pF	C_a =3297pF
Resonance frequency	1.266MHz	530kHz	392kHz	283kHz
Cp Measured	172.64pF	170.79 pF	159.57pF	158.07pF
Cp in 1X	64.93 pF	63.08 pF	51.86 pF	50.36 pF

Table 4.2: In 1X

Value	No C_a	C_a =814.3pF	C_a=1637pF	C_a =3297pF
Resonance frequency	1.728MHz	552 kHz	400 kHz	286.5 kHz
Cp Measured	92.65 pF	93.837 pF	83.94pF	74.166pF
Cp in 10X	77.23 pF	78.417 pF	68.52 pF	58.746 pF

Table 4.3: In 10X

The same experiment has been conducted by varying different parameters and they have been tabulated in Appendix B.

4.2. Analysis

From the experimental testing, the following observations are made:

- The capacitance, when measured with 10x probe, shows a capacitance lower than that measured with 1x probe. This can be explained with the help of a tank circuit. From the circuits shown in Figure 4.9, represents the coil with the parasitic capacitance Cp, whereas Figure 4.9b represents the situation when a probe is used to measure the parasitic capacitance. The capacitance Ca depicts the total capacitance at the probe tip.

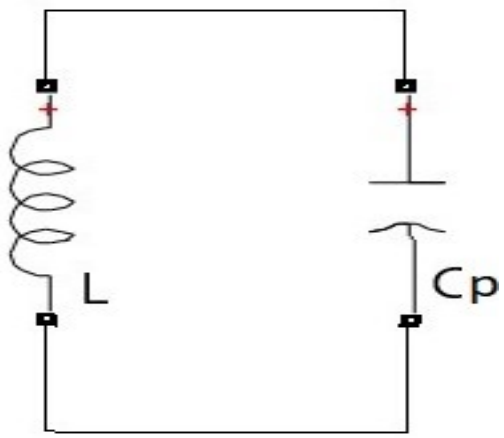

(a) Tank circuit

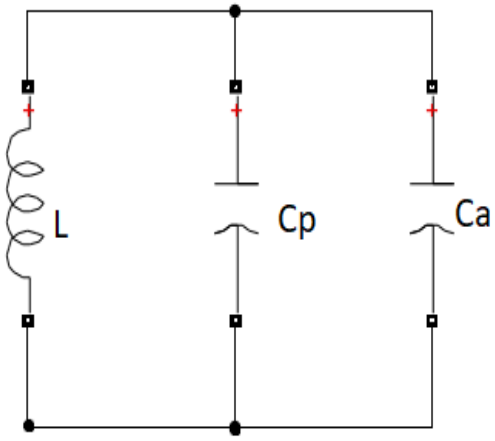

(b) Tank circuit with Probe

Figure 4.9: Representation of Probe capacitance

If we simply compare the resonant frequencies of Figure 4.9a and Figure 4.9b , we get $\omega_1 = \frac{1}{\sqrt{L \times C_p}}$ and $\omega_2 = \frac{1}{\sqrt{L \times (C_p + C_a)}}$. If f is a factor of by which ω_1 and ω_2 are related ,we can say;

$$f = \frac{\omega_2}{\omega_1} = \sqrt{\frac{C_p}{C_p + C_a}} \tag{4.11}$$

We know that in 10x, the induced capacitance and loading is less than that at 1X. Hence when at 10x, C_a is less than at 1x. So at 10x, f would be greater than at 1x, as can be seen from Equation 4.11. This can be a reason why the probe at 10X measures a capacitance lower than at 1X.

With the analysis, we can arrive at the answers of a few research questions:

For testing the high voltage insulation samples, the range of frequency and the highest voltage over which testing needs to be performed has to be decided. Based on these parameters, capacitance of the load has to be decided, taking into consideration the source that is available. With these three values confirmed, the range over which the inductance would be varied can be calculated. This will lead to analysing the resistance and the parasitic capacitance of the coil and methods to minimize these values. These are the essential calculations which will determine the design of the series resonance circuit.

The essential elements therefore, are the capacitance of the test object and the inductor that will be designed. In this thesis, as discussed in Chapter 2, the inductor will be varied based on the decided frequency and test object. The resistance and the capacitance that occur with the inductance influence the performance of the circuit which should be taken into account before getting into testing the samples. The resistance leads to drawing more current and heating losses. Two reasons besides the coil geometry which lead to additional resistance are the usage of a core to increase inductance and increase in frequency which lead to additional AC resistance. Methods to reduce the resistance have also been suggested in Chapter2. The other parameter, parasitic capacitance, which occurs based on the inductor geometry determines the self-resonance frequency of the coil. As seen before, this value difficult to measure due to the influence of measuring equipment and surroundings. Operating the circuit close to the self-resonant frequency can render it useless as resonance is not occurring in between the designed inductor and test object. When the value of parasitic capacitance is known it is recommended to operate the resonance circuit much farther from this frequency.

To get a precise measurement of the parasitic capacitance, a suggestion is to use a probe with as less capacitance as possible. The values of capacitance in the probe and their effect on measurement is mentioned in the previous section. The value can also be measured by varying a few parameters externally, such as, adding different values of external capacitance. To read the frequency more accurately, which determines the parasitic capacitance, the Fourier transform of the waveform can be taken, using the oscilloscope or in MATLAB.

5

Experimental Insulation Testing

This chapter starts with the testing of the insulation sample. For the range of 50 Hz to 1.6 kHz, the insulation samples is tested using an amplifier to observe the time to breakdown at different frequencies. The procedure followed for this experiment is also explained.

5.1. Test set up and Procedure:

Samples of oil paper insulation were used to test for their time to break down, with a set up as shown in fig. 5.1

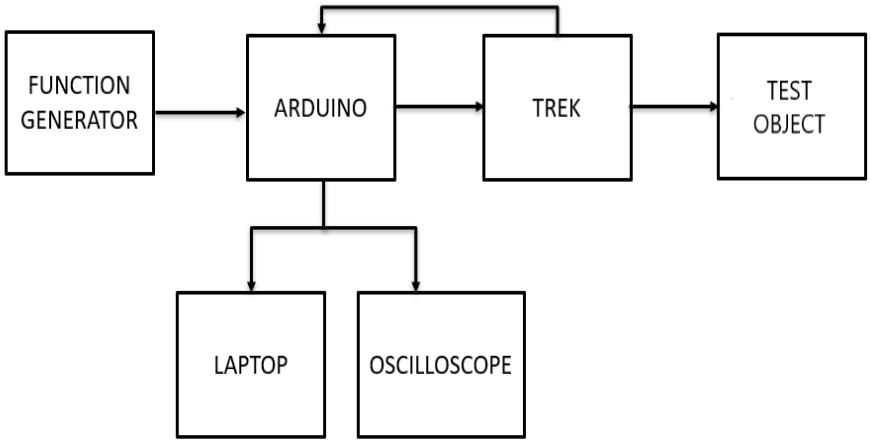

Figure 5.1: Schematic for Experiment

A ramp signal was used for amplitude modulation of sine waves which was given to the amplifier. The amplifier steps up the voltage at the input by 30kV. The frequency of the sine wave is varied to and the time to breakdown of each sample is noted. At each frequency, 10 samples are tested. The signal from the function generator is taken through an arduino for the following reasons:

- If the signal is supplied directly through a function generator, after every breakdown, the signal does not start from zero because the function generator continuously keeps producing the signal. This destroys the purpose of the experiment as each sample will be stressed differently.

- The arduino can be programmed to return the exact time of breakdown.

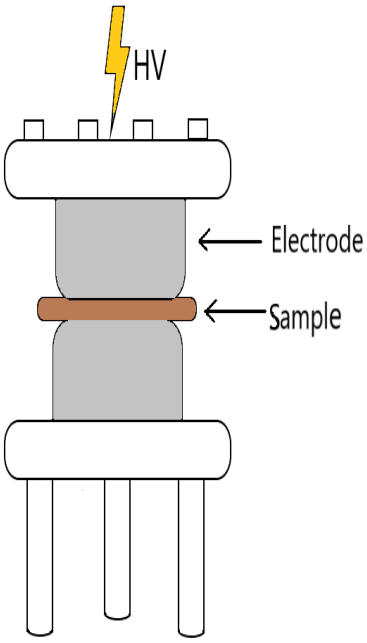

Figure 5.2: Sample for Testing

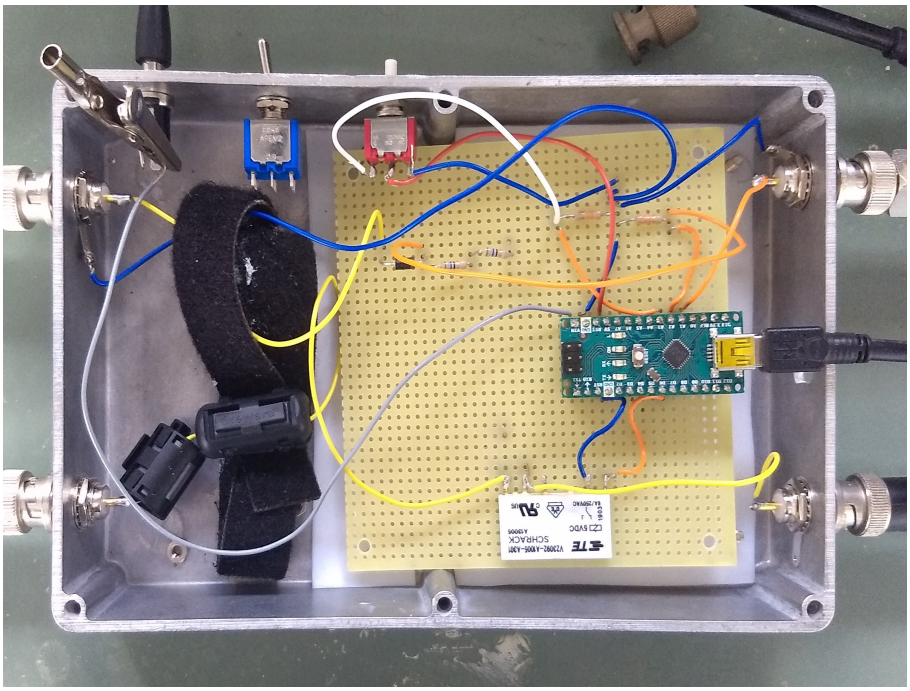

Figure 5.3: Interfacing with Arduino for suitable input waveform

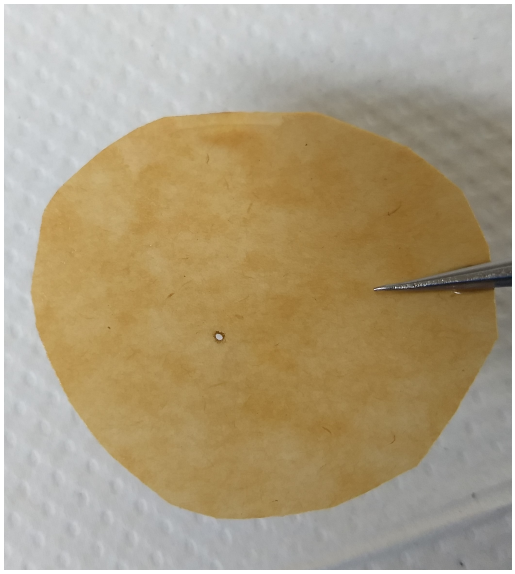

(a) Sample breakdown with one layer of insulation

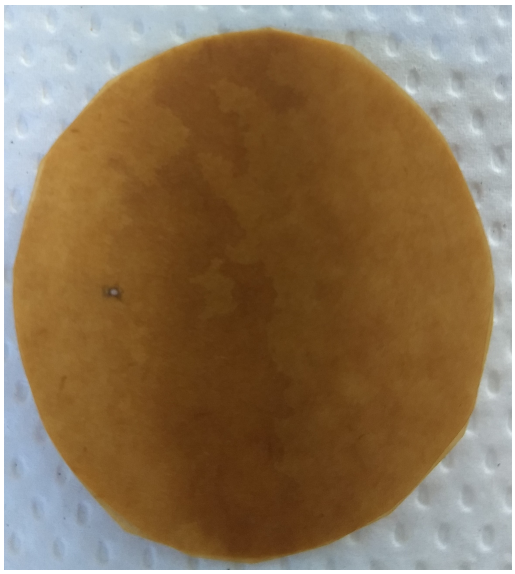

(b) Sample breakdown with two layer of

Figure 5.4: Insulation Sample after breakdown

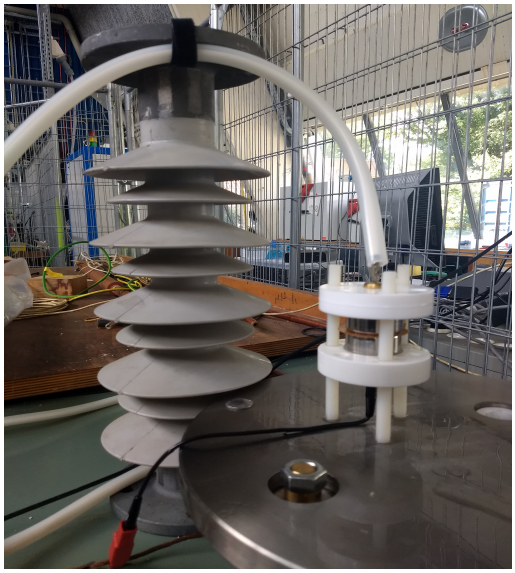

(a) Set up of Test sample for testing

(b) Set up connected to amplifier

Figure 5.5: Test object connection with amplifier

5.2. Breakdown testing:

The oil paper insulation samples of 150μm thickness, are tested for their time to breakdown by generating an amplitude modulated ramp signal of 1kV/s, which was applied to the sample. When the sample would breakdown, the time instant and applied voltage was noted to obtain the field

strength. With the data obtained from this test, the breakdown time was plotted to see if it could be analysed as a Weibull distribution [36].

The wave-forms in Figure 5.6 shows the breakdown as the current detected from the amplifier drops to zero. In each image, the blue and the pink wave forms, are the voltage reading from Trek amplifiers voltage divider and, the voltage after the diode; pick up some disturbance and noises just before the breakdown. The waveform during the breakdown was captured for many more samples, similar to the figures shown below. It can be concluded that the majority of breakdowns (between 50% - 60%) occur at the peak value of voltage, that is, under maximum stress. However, it is also interesting to see , that this is not the case through out. A number of breakdowns occur in during the rise or the fall in the sine wave, even when the stress is not the highest. Hence it can be seen that breakdown occurs, not only as an immediate effect of high stress, but can occur at other instances, due to a cumulative effect of high stress.

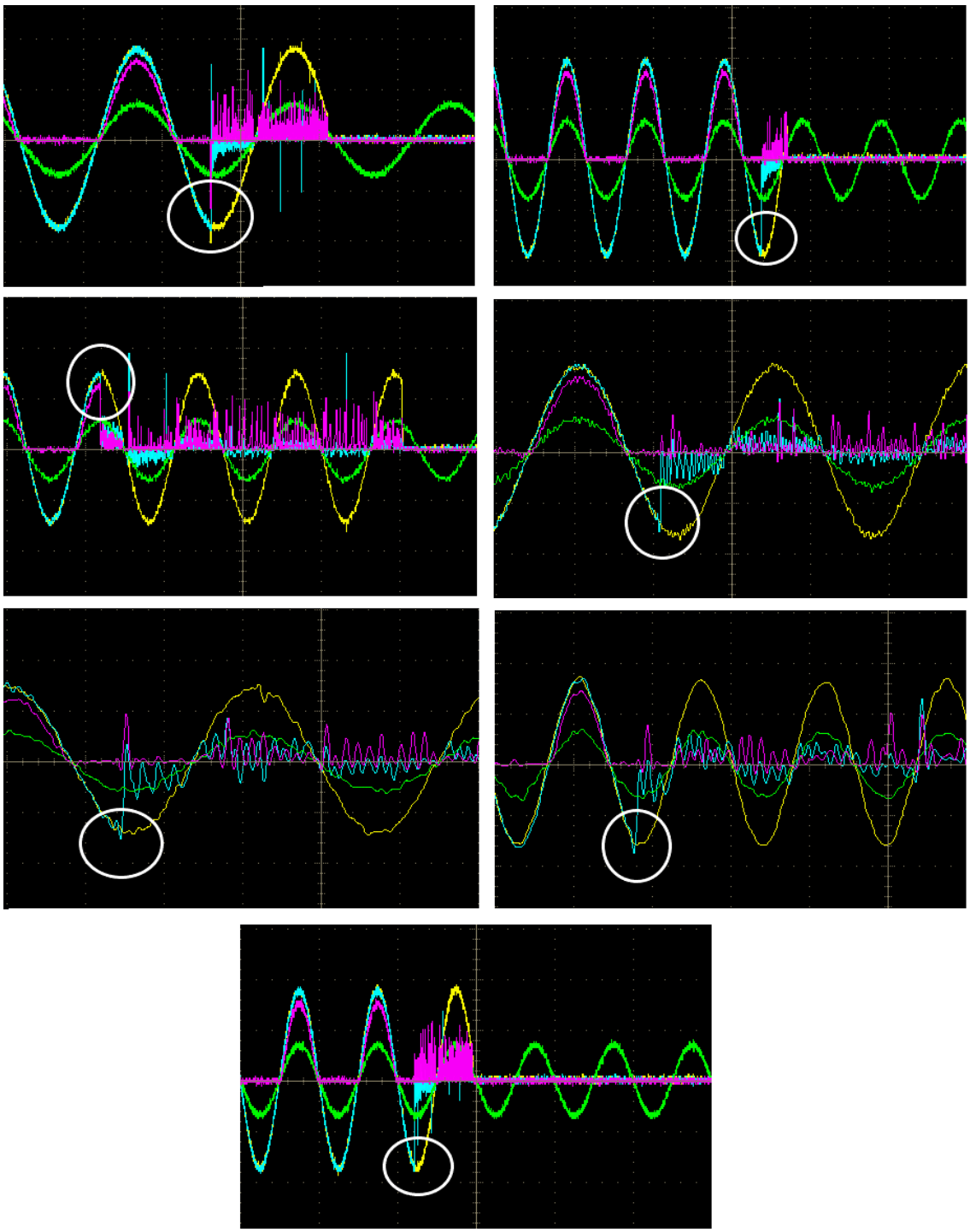

Figure 5.6: Wave forms at instant of breakdown

The test was performed with one layer of insulation and then with two layer of insulation samples.

5.3. Life time testing:

Secondly, the samples of insulation were tested to understand the process of ageing. after the time to breakdown test, when we know the stress at which the breakdown occurs, we tested 12 samples under lower stresses,by reducing about . The time taken for breakdown was noted. Successively, the voltage was lowered a few volts and 12 samples were tested again. This was done till a voltage was reached where the time to breakdown was very large for measurement during the current scenario. This procedure was repeated for the frequencies 400 Hz and 1600 Hz.

6

Results

This chapter presents the results obtained from the experiments which have been explained in chapter 5. The data obtained from those experiments have been plotted and analysed to understand the effect the high frequency signals have on the insulation samples.

6.1. Insulation testing and time to breakdown

Samples of oil paper insulation were testes under the set up and procedure described in chapter 5. With the data obtained from this test, the breakdown time was plotted to see if it could be analysed as a Weibull distribution.

6.1.1. Weibull analysis:

Life time and ageing test should technically be carried on for a wide range of time, going from seconds to at least many hours. Hence these tests present us with a result which is in the form of a wide scatter. For such data, Weibull analysis is considered a effective statistical tool for representation. For duration testing, Weibull analysis is based on the probability P, that an unbroken sample, breaks within the time span Δt [37]. Hence for duration tests, the probability

is expressed as :

$$P(t) = 1 - exp(-(\frac{t}{t_o})^m) \tag{6.1}$$

$$log(-log(1 - P(t))) = mlog(t) - mlog(t_0) \tag{6.2}$$

Generally, for plotting purposes, double logarithm is taken to obtain eq. (6.2) which basically becomes of the slope-intercept form$y = mx + C$.Here, the parameter $t_o$is the scale parameter and m is the shape parameter [[38]. When the data is to be evaluated based on the electric stress or voltage required for breakdown, the breakdown stress or voltage is entered as the x axis instead of time, the equation used is :

$$P(u) = 1 - exp(-(\frac{u}{u_o})^b) \tag{6.3}$$

Here, the electric field strength can also be used instead of voltage. In eq. (6.3), b is the shape parameter and u_o is the scale parameter [39]. The shape parameter is mainly the slope of the plot and the scale parameter is the point where the probability reaches 63.2 %. It denotes the average life time in the endurance test or the characteristic breakdown strength.

6.1.2. Test Results and Discussion:

The following graphs present the breakdown time taken by testing single layer and two layers of oil-paper insulation samples:

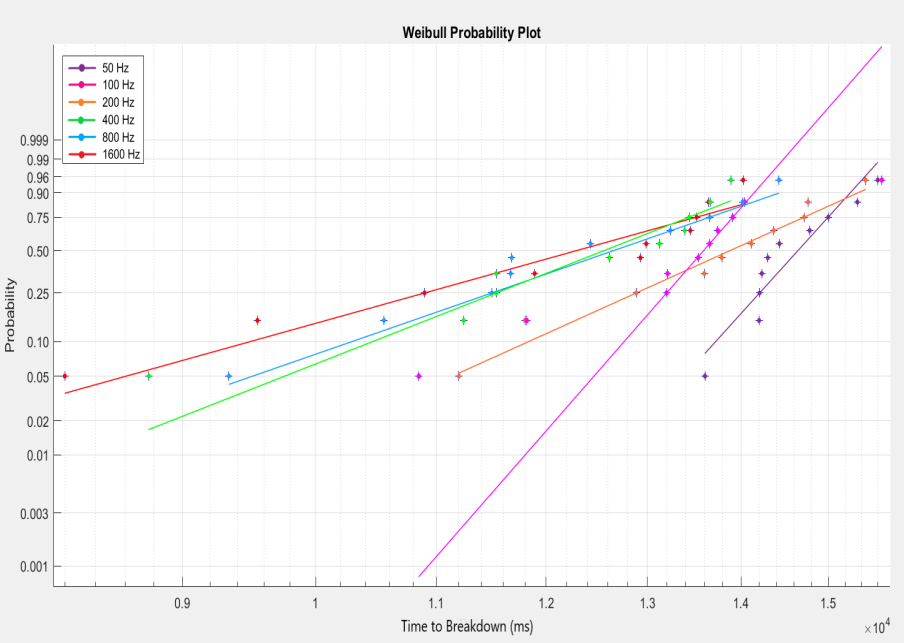

Figure 6.1: Weibull analysis of time to breakdown with 1 samples

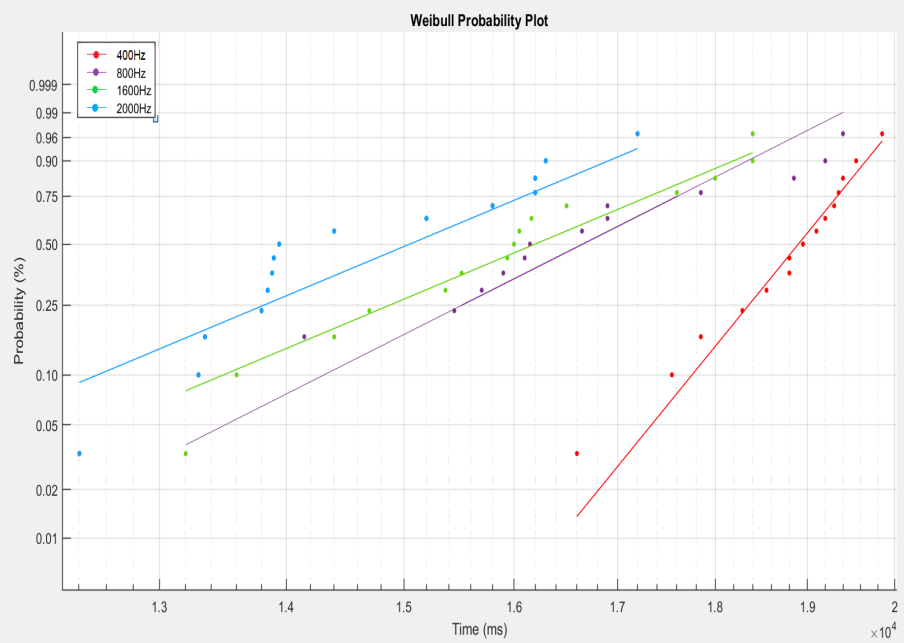

Figure 6.2: Weibull analysis of time to breakdown with two samples

When testing one layer of insulation, the samples could only be tested up till 1600 Hz as above that frequency, the current limit of the amplifier was exceeded. However, with 2 layers of insulation it was possible to test till 2000 Hz till the amplifier tripped because of over current.

In Figure 6.1, it can be seen that the plot for some frequencies show irregularities. The graph obtained from testing two layers is clearer and we are able to observe an increase in frequency also leads to an increased probability of an early breakdown. This trend is not very evident in Figure 6.1. Moreover,even in Figure 6.2, we observe that some of the points do not coincide with the solid line graph. These graphs basically work as a comparison of the collected data with a predicted Weibull distribution. This is mainly because such tests are normally performed by testing a higher number of samples. Due to shortage of time this test was performed only using 10 samples for each test which ultimately gives as only an idea of the nature of the result.

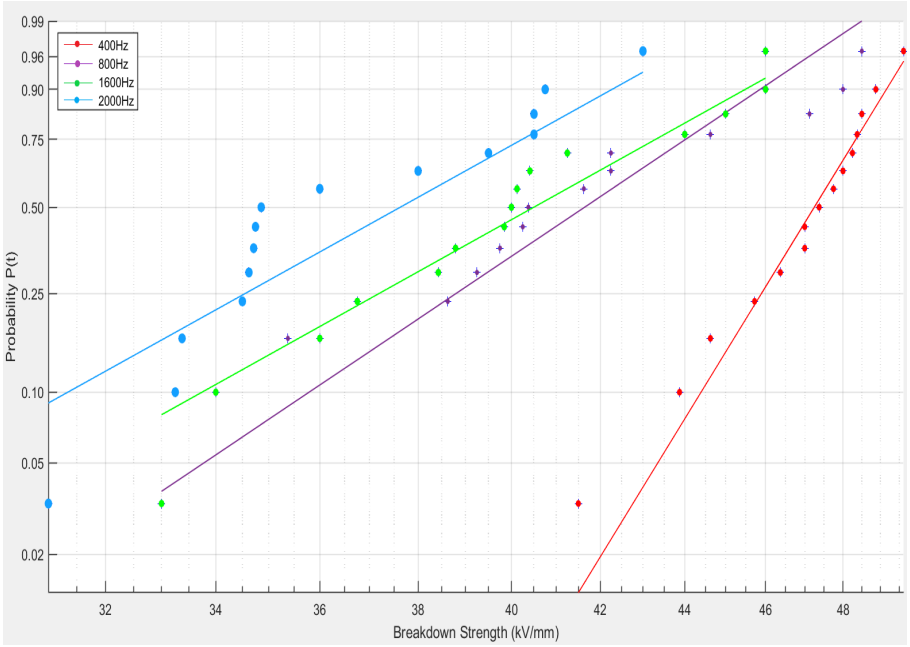

Figure 6.3: Weibull analysis of breakdown strength of two samples

Based on the time to breakdown we also get the values of breakdown strength. The Figure 6.3 shows the Weibull plot of breakdown strengths at different frequencies, using 2 layer of insulation. Here we see that with the increase in frequency, the probability of the insulation sample to breakdown increases even at a reduced stress. The same trend can be seen in the bar graphs representing the time to breakdown in Figure 6.4 and Figure 6.5 where we are also able to see the standard deviation.

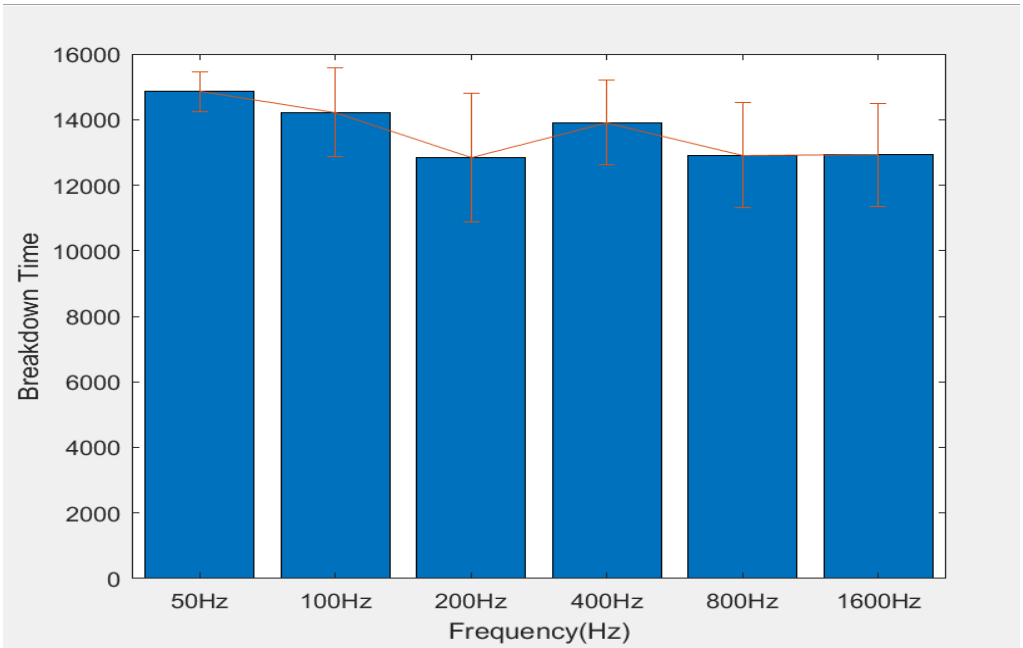

Figure 6.4: Scale parameter (η) of oil-paper samples (1 Layer) as a function of voltage frequency including standard deviation

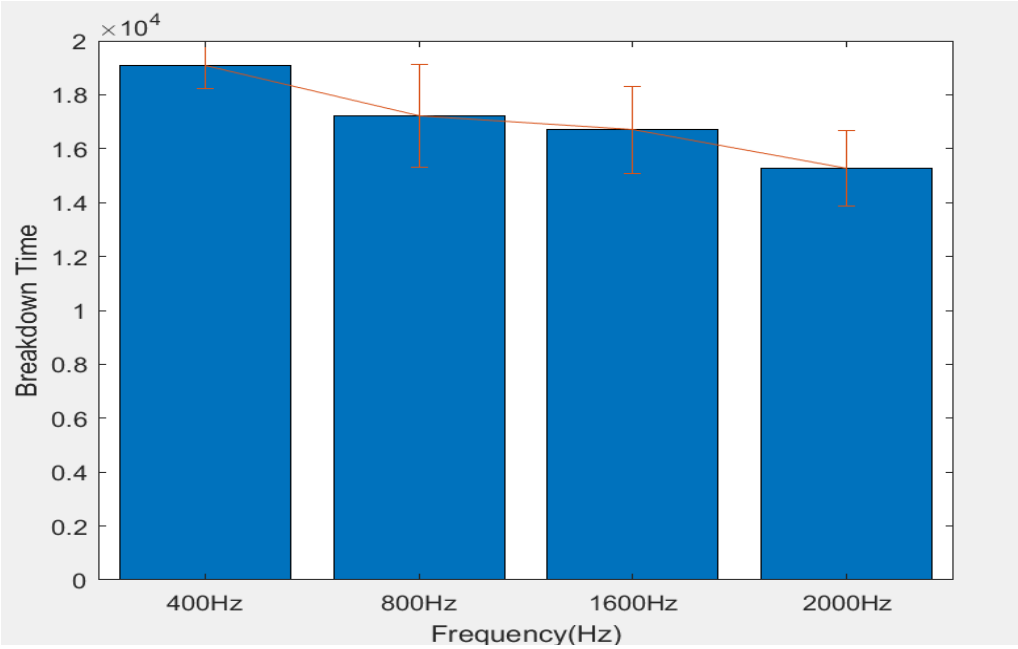

Figure 6.5: Scale parameter (η) of oil-paper samples (2 Layer) as a function of voltage frequency including standard deviations

After noting the time to breakdown of samples at selected frequencies, two frequencies

were selected to study the aging of sample under different frequencies. Figure 6.6 and Figure 6.7 show the graphs plotted after studying the breakdown of insulation at different voltage stresses. Figure 6.6 is plotted by taking the median of the time to breakdown obtained at each voltage. Figure 6.7 is plotted based on the mean of the values obtained at each voltage. It can be seen that when using the median, there is a similar trend in both frequencies, 400 Hz and 1600 Hz, that, with decrease in voltage applied, time to breakdown increases. This is also evident in the 50 Hz aging curve that is already available, that time to breakdown decreases with increase in stress. When the mean is used as a tool to plot the graph, we see the plots behaving opposite to each other, one displays a positive slope while the other has negative one. A possible reason for this can be because, while testing for the time to breakdown at different voltages, certain samples end up taking an unpredictable amount of time. When taking the mean, all the values equally influence the result, which is not the case with taking the median.

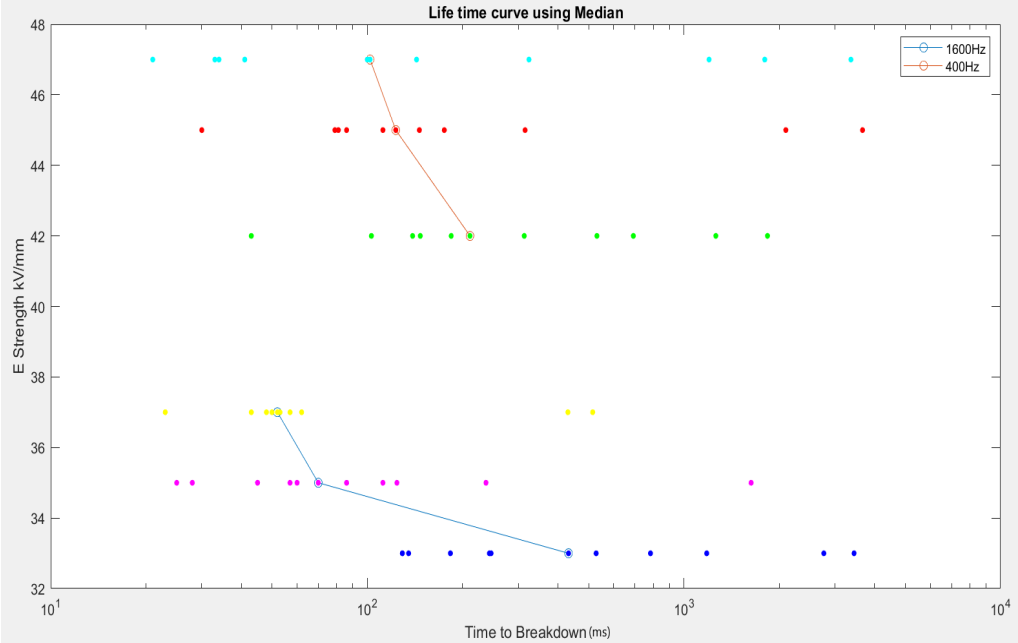

Figure 6.6: Life time Curve Using Median

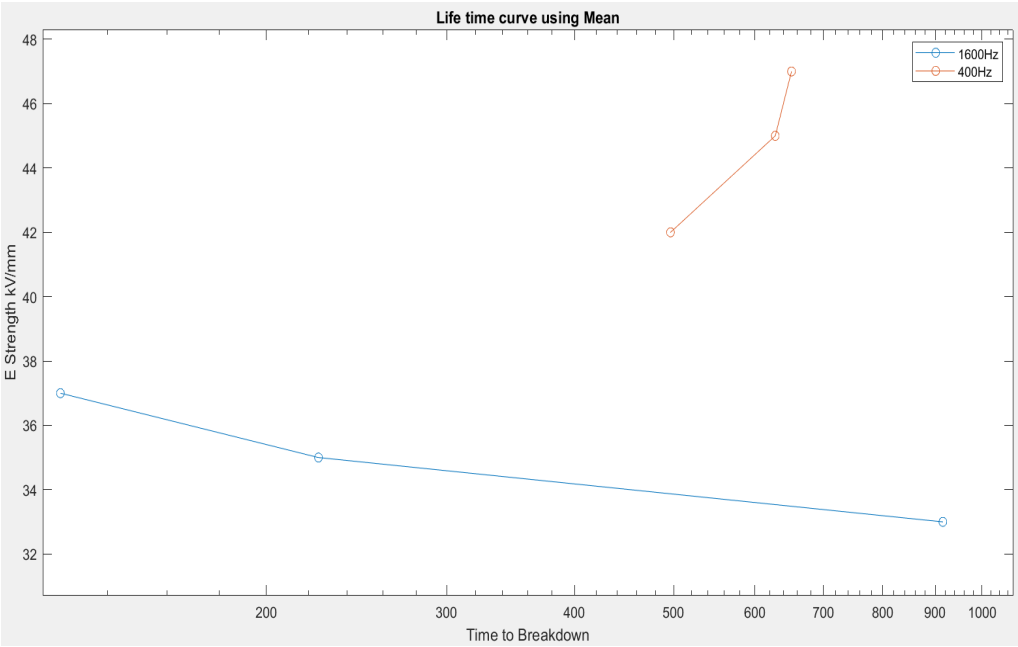

Figure 6.7: Life-time Curve Using Mean

Frequency	Scale Parameter	Shape Parameter	CI Lower Limit	CI upper limit
50 Hz	14855.014	26.11	1448.5 , 41.53	1523.4 , 16.41
100 Hz	14222.21	13.71	13563.09 , 8.27	14913.36 , 22.75
200 Hz	12853.65	9.16	11978.91 , 5.31	13792.27 , 15.78
400 Hz	13904.87	12.19	13177.84 , 7.71	14672.01 , 19.29
800 Hz	12916.62	9.54	12061.74 , 5.80	13832.07 , 15.69
1600 Hz	12924.88	11.65	12227.82 , 6.85	13661.68 , 19.83

Table 6.1: Shape and Scale parameters with Confidence Interval for 1 layer of insulation

Frequency	Scale Parameter	Shape Parameter	CI Lower Limit	CI upper limit
400 Hz	19099.25	31.38532343	18779.59 , 20.69	1942.4 , 47.5941
800 Hz	17223.25	9.95	1632.04 , 6.736	1817.604 , 14.683
1600 Hz	16701.77	11.41	1593.62 , 7.7124	1750.41 , 16.89
2000 Hz	15280.15	11.51	1458.4 , 7.84	1601.0 , 16.91

Table 6.2: Shape and Scale parameters with Confidence Interval for 2 layer of insulation

The table 6.1 and table 6.2 tabulate the shape and scale parameters of the data, which is the time to breakdown. The shape parameter determines the slope of the curve and the scale

parameter is defined at the point in time when the probability of breakdown reaches 63.2%. In the last two columns of the table we also see CI lower and upper bound, which are the confidence interval of the data. What this interval tells us is the area, within which 95% probability of breakdown lies. The lower limit is given as minimum (scale, shape) parameter and upper limit is given as maximum (scale, shape) parameter. This interval is specifically important when the samples tested are very few to form conclusive results.

6.2. Insulation testing conclusion:

Based on the results obtained from insulation testing, we can arrive at some answers for the questions formed in chapter 1.

The test set up was discussed in chapter 5, was used to conduct the describes experiments and the data obtained was analysed. The graphs plotted show that the insulation material breaks down faster, at a higher frequency. Along with this, one very important factor about testing is that it is better to draw conclusion when the number of samples tested is large, which is explained through Figure 6.1. When testing using one layer of insulation, we come across a few abnormalities where the time to breakdown does not follow the general trend.

From the lifetime curve, it can be seen that the sample breaks down faster at a higher frequency and as voltage or electrical stress increases. With the available data, it can already be said that high frequency signals have an adverse effect on the insulation ageing. This must be taken seriously as power electronic devices becoming increasingly common. Problems can be avoided by redefine lifetime curves, hence a more accurate prediction towards insulation failure. For deeper understanding of how the high voltage insulation would be affected during operation, testing these insulation under a combination of high frequency signals would be helpful. With further research in the field of power electronics, it might also be possible to reduce these harmonics to a certain level, while achieving the desired results. It would, although be nearly impossible to put a stop to absolutely all high frequency harmonics and hence to some degree, the insulation material will be affected. Updated testing procedure and accurate prediction of failure ensure better preparedness.

7

Reflection

The original idea behind this project was mainly, to attain a complete model using which insulation testing at high voltage at high frequency could be greatly simplified. It was supposed to be a model which would contain life time or aging data of a high voltage insulation at different frequencies so that, depending on the magnitude at which different frequencies occur, their share on aging the insulation can be deciphered. Ideally, this would be the most flexible method to study insulation aging as this can be varied and applied to any kind of high frequency disturbance.
As beautiful as the thought behind it is, it would be fair to say, I think, that it is slightly ambitious to achieve is the duration that was provided. At least at my level of experience, this is my humble opinion. Added to that, the unavoidable lockdown pushed the desired conclusion even further. With a drastic shrinkage in the available time to experiment, focus had to be shifted to things that could be done at home. Looking at what we want to achieve with this thesis, it was obvious that most of it could only be done through experiments and lab work. Hence, evaluating the difficulties and issues we had faced so far, during the experimental work, a few more aspects to investigate were added to the project. These involved

- Design parameters to be considered while making a high frequency inductor

- Influence of parasitic capacitance on an inductor and resonance circuit's performance.

- Ways to reduce losses in an inductor.

8

Conclusion and Recommendation

The goal of this research is to investigate the effect that high frequency harmonic signals have on the high voltage insulation. Currently, the only lifetime curves available are for 50Hz signals, which is used as reference for insulation aging. However, to reach our goal, we aim to produce similar life time curves for a range of frequencies. This will help in determining the contribution of an individual high frequency signal in insulation breakdown, or failure. To test insulation samples at high voltage and at high frequency, a specific set up needs to be designed such that the frequency can be varied. To a certain limit, a high-power amplifier can be used. This currently, could not be used for the entire range of frequencies as, the performance of amplifier is limited by the current and since the range of frequency being tested is wide, one amplifier cannot satisfy the entire process of testing. Therefore, the aim of the thesis is:

- To study the effect of high frequency signals on high voltage insulation material with the help of life time curves.

- For the testing, a thorough investigation needs to be done on the circuit requirements for testing.

These goals will be achieved by answering the following research questions,

- What is the appropriate set up to test an insulation sample under high voltage and high frequency such that the frequency can be varied for each test?

- What calculations and criteria are required to decide on an appropriate circuit for testing?

- What are the fundamental elements of the selected test circuit,how do these elements influence its performance and how accurate can they be measured?

- When insulation is tested for breakdown using a high power amplifier, what conclusions can be drawn about the aging of the insulation and its lifetime.

8.1. Conclusion:

The objective of the thesis to investigate the effect that high frequency harmonic signals have on the high voltage insulation with the help of life time curves and a thorough investigation on the circuit requirements for testing is partially met. Based on the research done during this thesis, the conclusions that can be drawn based on the research questions are as follows:

- A set up to test an insulation sample under high voltage and high frequency, such that the frequency can be varied for each test, is proposed in chapter 5. Special attention has to be paid to ensure uniform application of electric stress on the surface of the sample and sharp edges are avoided to avoid field concentration. When testing for time to breakdown, it is important to use a method such that the function is always started from 0, for each sample. The function generator used is suitable till 1.6 kHz. Another method to perform the experiments is with he use of a series resonance circuit with a variable inductor has been suggested.

- For testing the high voltage insulation samples with a resonance circuit, the range of frequency and the highest voltage at which testing needs to be performed has to be decided., as well as the capacitance of the load. With these three values confirmed, the range over which the inductance of the coil has to be varied can be calculated.

- Analysis of the parameters resistance and the parasitic capacitance of the coil and methods to minimize these values are essential to determine the design of the series resonance circuit.

The resistance leads to drawing more current and heating losses. The other parameter, parasitic capacitance, which occurs based on the inductor geometry determines the self-resonance frequency of the coil. The parasitic capacitance is difficult to measure due to the influence of measuring equipment and surrounding. To get a precise measurement of the parasitic capacitance, a suggestion is to use a probe with as little capacitance as possible. Operating the circuit close to the self-resonant frequency can render it useless as resonance is not occurring between the designed inductor and test object. it is recommended to operate the resonance circuit far from the self-resonance frequency.

- Due to COVID19 circumstances only a limited number of insulation breakdown measurements were performed. The graphs in Figure 6.1 and Figure 6.2 show that the insulation material breaks down faster, at a higher frequency. Along with this, one very important factor about testing is that it is better to draw conclusion when the number of samples tested is large. When testing using one layer of insulation a few abnormalities where found where the time to breakdown does not follow the general trend.

8.2. Recommendation:

- Designing the coil and implementing it in a suitable circuit: Based on the methods and planning described in chapter 2 , chapter 3 and chapter 4, circuit simulation and practical experiments can be done to create a high frequency inductor suitable fora series resonance circuit. Decisions regarding the number of turns or selection of core can be made based on the voltage ad frequency of operation. Winding an actual inductor and using it with a load capacitance will be the next step towards getting a high voltage high frequency source for testing insulation samples.

- Testing with more number of samples: the testing done in this thesis has used 10 samples of insulation for each frequency. For drawing a lifetime curve, however, it is recommended that the same experiments be carried out using a larger umber of samples. Once the samples are tested, the suggestion is to draw the lifetime curves using mean and median and compare the results with the graphs provided in chapter 6.

- Superimposing two frequencies (or overlapping with DC) for testing: The samples tested have only been tested under a single frequency. Most often, when a high voltage equipment is under operation, harmonics of different frequencies act on it. In chapter 1 of this thesis, a few studies have also suggested testing insulation on high frequency with the fundamental

frequency. For future testing, this would be a good direction to proceed in.

- Effect of combined harmonics of different frequencies: If this experiment is taken ahead and life time curves at different frequencies are obtained, it would be beneficial to come up with a mathematical model or method such that different frequencies can be combined based on the stress the apply on the insulation and their combined effect can be seen.

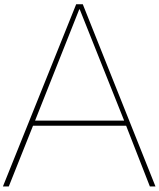

Appendix-1

This appendix contains the working behind the calculation of mutual and Maxwell's capacitance matrix through Software such as COMSOL.

The Maxwell's capacitance matrix is derived by the procedure below: Consider a system of n conductors. Supposing all conductors to be free of insulated, free of charge and at zero potential initially, a unit charge given to one conductor will increase its own potential,by say p_{11} and its surrounding conductors, by p_{1n}. p_{11} can be called the potential coefficient of of the conductor on itself, while p_{1n}, will be the potential coefficient of the first conductor on all the other conductors. With the same logic, if instead of a unit charge, a charge Q_1 is given to the conductor, the voltage of each conductor will become:

$$V_1 = p_{11}Q_1 \text{ , } V_2 = p_{12}Q_1 \text{ ,..., } V_n = p_{1n}Q_1$$

If the first conductor is now completely discharged and another conductor is given the charge, say Q_2, now this will raise the potential of the charged conductor by p_{22} and the remaining conductors by p_{2n}.

Similarly, if charge Q_n is given to the nth conductor, then the potential on each conductor becomes:

$V_1 = p_{n1}Q_n$, $V_2 = p_{n2}Q_n$,..., $V_n = p_{nn}Q_n$

Based on the above principles, the electrical potentials in such a system can be depicted with the following equations

$$V_1 = p_{11}Q_1 + p_{21}Q_2 + \ldots + p_{n1}Q_n \quad \text{(A.1)}$$

$$V_2 = p_{12}Q_1 + p_{22}Q_2 + \ldots + p_{n2}Q_n \quad \text{(A.2)}$$

.
.
.

$$V_n = p_{1n}Q_1 + p_{2n}Q_2 + \ldots + p_{nn}Q_n \quad \text{(A.3)}$$

where, V_n is the potential of the n^{th} conductor. Therefore, for n number of conductors, there are n equations with n^2 number of potential coefficients.

The above equations can be solved to get the charges $Q_1, Q_2 \ldots Q_n$. The equations become:

$$Q_1 = c_{11}V_1 + c_{12}V_2 + \ldots + c_{1n}V_n \quad \text{(A.4)}$$

$$Q_2 = c_{21}V_1 + c_{22}V_2 + \ldots + c_{2n}V_n \quad \text{(A.5)}$$

.
.
.

$$Q_n = c_{n1}V_1 + c_{n2}V_2 + \ldots + c_{nn}V_n \quad \text{(A.6)}$$

The co-efficient of these equations, i.e. c, is called the coefficient of induction. Out of these coefficients, the coefficient c_{11} is the quantity of charge on the first conductor when it has a potential of unity and all the other conductors are at 0. This is termed as the capacity of that specific conductor and it depends on the form and the potential on all conductors of the system.

The remaining coefficient, of the form c_{lm} represent the charge on the l^{th} conductor due to the unity potential on the m^{th} conductor. The Maxwell's capacitance can be depicted as :

$$\begin{pmatrix} Q_1 \\ Q_2 \\ . \\ . \\ Q_n \end{pmatrix} = \begin{bmatrix} c_{11} & c_{12} & \dots & c_{1n} \\ c_{21} & . & \dots & c_{2n} \\ . & . & . & . \\ . & . & . & . \\ c_{n1} & c_{n2} & \dots & c_{nn} \end{bmatrix} \begin{pmatrix} V_1 \\ V_2 \\ . \\ . \\ V_n \end{pmatrix}$$

The above matrix yields the equation:

$$Q_1 = c_{11}V_1 + c_{12}V_2 + \dots + c_{1n}V_n \tag{A.7}$$

We know that by considering the mutual capacitance, that is, the capacitance induced between conductors and between conductor and ground, we have the total charge on a conductor as :

$$\begin{aligned} Q_1 &= C_{m11}V_1 + C_{m12}(V_1 - V_2) + \dots + C_{m1n}(V_1 - V_n) \\ &= (C_{m11} + C_{m12} + \dots + C_{m1n})V_1 - C_{m12}V_2 - \dots - C_{m1n}V_n \end{aligned} \tag{A.8}$$

Comparing Equation A.7 and Equation A.8, we find that in the matrix, $c_{11} = (C_{m11} + C_{m12} + \dots + C_{m1n})$, which is also how we explain c_{11}, in the derivation [40]. Hence, to switch between Maxwell's and mutual capacitance matrix, we can use:

$$\begin{pmatrix} Q_1 \\ Q_2 \\ . \\ . \\ Q_n \end{pmatrix} = \begin{bmatrix} \sum_{i=1}^{n} C_{m,1i} & -C_{m12} & \dots & -C_{m1n} \\ -C_{m21} & . & \dots & -C_{m2n} \\ . & . & . & . \\ . & . & . & . \\ -C_{mn1} & -C_{mn2} & \dots & \sum_{i=1}^{n} C_{m,ni} \end{bmatrix} \begin{pmatrix} V_1 \\ V_2 \\ . \\ . \\ V_n \end{pmatrix}$$

B

Appendix-2

In chapter 4, a table was shown for the experimental measurement of parasitic capacitance of a coil. The same experiment was also done by varying the resistance and the frequency of the supply voltage. The results are presented in the table below.

Measured at : 10V peak to peak, 10Hz, R=5.602kΩ, L= 105.51 H

Value	No C_a	C_a=559.2pF	C_a=1637pF
Resonance frequency	1.67 MHz	617 kHz	378 kHz
Cp	86.39 pF	72.5 pF pF	31pF
Cp in 10X	70.97pF	57.08 pF	15.58 pF

Variable Resistance:

Measured at : 10V peak to peak, 10Hz, No added capacitance

Value	R= 5.602 KOhm	R= 100.04 KOhm	R= 10.059 MOhm
Resonance frequency	1.266MHz	1.283 MHz	1.2915 MHz
Cp	172.64pF	170.1pF	167.90 pF
Cp in 10X	64.93 pF	62.39 pF	60.19 pF

Varying source voltage : No change is observed Varying Frequency: C=3297 pF, R=5.602kOhms

Resonance frequency	Fs=10Hz(1X)	Fs=100Hz(1X)	Fs=10Hz(10X)	Fs=100Hz(10X)
Cp	283kHz	283kHz	286.5kHz	286.5kHz
Cp in 10X	158.07pF	158.07pF	74.166pF	74.166pF

Bibliography

[1] N. Jaalam, N. Rahim, A. Bakar, C. Tan, and A. M. Haidar, "A comprehensive review of synchronization methods for grid-connected converters of renewable energy source," Renewable and Sustainable Energy Reviews, vol. 59, pp. 1471 – 1481, 2016.

[2] M. Knenicky, R. Prochazka, and O. Sefl, "Influence of nonstandard voltage stresses on transformer insulation paper," in 2017 IEEE Conference on Electrical Insulation and Dielectric Phenomenon (CEIDP), pp. 700–703, Oct 2017.

[3] S. Banerjee and S. H. Jayaram, "Performance of medium voltage cable terminations under high frequency voltage waveforms," pp. 538–543, July 2010.

[4] T. Van Craenenbroeck, J. De Ceuster, J. P. Marly, H. De Herdt, B. Brouwers, and D. Van Dommelen, "Experimental and numerical analysis of fast transient phenomena in distribution transformers," in 2000 IEEE Power Engineering Society Winter Meeting. Conference Proceedings (Cat. No.00CH37077), vol. 3, pp. 2193–2198 vol.3, 2000.

[5] K. O'Connell, Heating effects through harmonic distortion on electric cables in the built environment. PhD thesis, Technological University Dublin, 2013.

[6] N. Hardt and D. Koenig in Conference Record of the 1998 IEEE International Symposium on Electrical Insulation (Cat. No.98CH36239), vol. 2, pp. 517–520 vol.2, June 1998.

[7] T. Sels, J. Declercq, J. Lopez-Roldan, D. Vsn Dommelen, and R. Belmans, "The ageing of cast resin subject to repetitive combined voltages of low and high fundamental frequencies," in 39th International Universities Power Engineering Conference, 2004. UPEC 2004., vol. 1, pp. 133–137 Vol. 1, Sep. 2004.

[8] M. Ghassemi, "Accelerated insulation aging due to fast, repetitive voltages: A review identifying challenges and future research needs," IEEE Transactions on Dielectrics and Electrical Insulation, vol. 26, no. 5, pp. 1558–1568, 2019.

[9] L. Paulsson, B. Ekehov, S. Halen, T. Larsson, L. Palmqvist, A. . Edris, D. Kidd, A. J. F. Keri, and B. Mehraban, "High-frequency impacts in a converter-based back-to-back tie; the

eagle pass installation," IEEE Transactions on Power Delivery, vol. 18, no. 4, pp. 1410–1415, 2003.

[10] A. Cavallini, I. Ghinello, G. Maszanti, and G. C. Montanari, "Accelerated capacitor degradation due to non sinusoidal voltage supply and reliability of insulation systems," in 8th International Conference on Harmonics and Quality of Power. Proceedings (Cat. No.98EX227), vol. 2, pp. 720–726 vol.2, 1998.

[11] S. B. Warder, E. Friedlander, and A. N. Arman, "The influence of rectifier harmonics in a railway system on the dielectric stability of 33-kv cables," Proceedings of the IEE - Part II: Power Engineering, vol. 98, no. 63, pp. 399–411, 1951.

[12] M. Nagel, C. Herold, T. Wenzel, and T. Leibfried, "Combined high frequency and high voltage insulation system investigation," in Conference Record of the 2006 IEEE International Symposium on Electrical Insulation, pp. 440–443, June 2006.

[13] G. Reed, R. Pape, and M. Takeda, "Advantages of voltage sourced converter (vsc) based design concepts for facts and hvdc-link applications," in 2003 IEEE Power Engineering Society General Meeting (IEEE Cat. No.03CH37491), vol. 3, pp. 1816–1821 Vol. 3, 2003.

[14] M. Schueller, S. Ph, J. S, K. Ch, G. G, R. Christen, M. Bucher, and J. Smajic, "Development of a pulsed high frequency source for testing cellulosic insulation material for high voltage solid state transformer applications," pp. 1–4, 09 2018.

[15] T. Sels, J. Karas, J. Declercq, D. Dommelen, and R. Belmans, "Ageing of electrical insulation materials subject to fast transients using a tesla transformer," Proceedings of the Universities Power Engineering Conference, vol. 37, 01 2002.

[16] ISO Central Secretary, "High-voltage test techniques part 3: Definitions and requirements for on-site testing," Standard IEC 60060-3:2006(E), International Organization for Standardization, Geneva, CH, 2006.

[17] G. L. Piazza, R. L. Alves, C. H. I. Font, and I. Barbi, "Resonant circuit model and design for a high frequency high voltage switched-mode power supply," in 2009 Brazilian Power Electronics Conference, pp. 326–331, 2009.

[18] R. W. Erickson and D. Maksimović, Inductor Design, pp. 539–564. Boston, MA: Springer US, 2001.

[19] E. Snelling, Soft Ferrite - Properties and Applications. Ilife Books LTD, 1969.

[20] C. W. T. McLman, Transformer and Inductor Design Handbook. Marcel Dekker, Inc, 3rd ed., 2004.

[21] M. Bartoli, A. Reatti, and M. K. Kazimierczuk, "Modelling iron-powder inductors at high frequencies," in Proceedings of 1994 IEEE Industry Applications Society Annual Meeting, vol. 2, pp. 1225–1232 vol.2, 1994.

[22] A. Hilal and B. Cougo, "Optimal inductor design and material selection for high power density inverters used in aircraft applications," in 2016 International Conference on Electrical Systems for Aircraft, Railway, Ship Propulsion and Road Vehicles International Transportation Electrification Conference (ESARS-ITEC), pp. 1–6, 2016.

[23] S. Weber, M. Schinkel, S. Guttowski, W. John, and H. Reichl, "Calculating parasitic capacitance of three-phase common-mode chokes," 04 2020.

[24] M. S. Sanjari Nia, S. Saadatmand, P. Shamsi, and M. Ferdowsi, "Analysis of various transformer structures for high frequency isolation applications," 08 2019.

[25] J. KrishnanA, Parikshith B.C, "Analysis of flux fringing for high-frequency ac inductor design," September 2010.

[26] M. Zdanowski and R. Barlik, "Analytical and experimental determination of the parasitic parameters in high-frequency inductor," Bulletin of the Polish Academy of Sciences Technical Sciences, vol. 65, 02 2017.

[27] G. Grandi, M. K. Kazimierczuk, A. Massarini, and U. Reggiani, "Stray capacitances of single-layer air-core inductors for high-frequency applications," in IAS '96. Conference Record of the 1996 IEEE Industry Applications Conference Thirty-First IAS Annual Meeting, vol. 3, pp. 1384–1388 vol.3, 1996.

[28] A. Massarini and M. K. Kazimierczuk, "Self-capacitance of inductors," IEEE Transactions on Power Electronics, vol. 12, no. 4, pp. 671–676, 1997.

[29] D. Sinha, P. K. Sadhu, N. Pal, and A. Bandyopadhyay, "Computation of inductance and ac resistance of a twisted litz-wire for high frequency induction cooker," in 2010 International Conference on Industrial Electronics, Control and Robotics, pp. 85–90, 2010.

[30] A. Massarini, M. Kazimierczuk, and G. Grandi, "Lumped parameter model for single-and multiple-layer inductors," pp. 295 – 301 vol.1, 07 1996.

[31] J. C. Maxwell, A treatise on electricity and magnetism. Oxford : Clarendon Press, 1831-1879.

[32] D. Knight, "The self-resonance and self-capacitance of solenoid coils," 05 2010.

[33] Tektronix, Primerwww.tektronix.com/accessorie, ABCs of Probes, 2016.

[34] "Select the right oscilloscope probe for your application(white papers)," tech. rep., Ni.com, February 2020.

[35] UW–Madison Physics Department, Introduction to Oscilloscope Probes, 1 ed., 2009.

[36] "Electric cables - additional test methods," Harmonization Document HD 605 S2, CENELEC, rue de Stassart 35, B - 1050 Brussels, 2008.

[37] H. Jin, I. Tsekmes, J. Wu, A. R. Mor, and J. Smit, "The effect of frequency on the dielectric strength of epoxy resin and epoxy resin based nanocomposites," in 2017 International Symposium on Electrical Insulating Materials (ISEIM), vol. 1, pp. 141–143, 2017.

[38] F. Kreuger, Industrial High Voltage 4. Coordinating 5. Testing 6. Measuring. 1992.

[39] J. Wu, H. Jin, A. R. Mor, and J. Smit, "The effect of frequency on the dielectric breakdown of insulation materials in hv cable systems," in 2017 International Symposium on Electrical Insulating Materials (ISEIM), vol. 1, pp. 251–254, 2017.

[40] D. Lorenzo, "White paper: The maxwell capacitance matrix," Tech. Rep. WP110301, FastFieldSolver, East Lansing, Michigan, March 2011.

Acknowledgement

Since coming to the Netherlands, I had the pleasure of meeting many interesting people. Together with their support and that of my friends and family abroad, this thesis would not have been possible.

First of all, I would like to thank professor Peter Vassen, for providing me with the opportunity to do a project under his guidance. I also want to thank him for his for introducing me around to many test engineers at KEMA who had a lot of experience in the field of high voltage testing and cable testing.

I am very grateful to professor Mohamad Ghaffarian Niasar, for putting together such an interesting project and allowing me to work on this idea for my thesis. I specially would like to thank him for his regular supervision of my work and his constant support and feedback throughout the duration of my work.

My gratefulness lies also with the staff of the HV lab: Mr. Radek Heller, Mr.Luis Heredia, Mr.Paul Van Nes and Mr.Wim Termorshuizen. Thanks to your in depth knowledge and thoughtful guidance, my time in the lab was very enjoyable.

I would also specially like to thank Ms.Hong He, from KEMA laboratories for sharing her amazing experience in testing high voltage cables and being readily available whenever I was confused and required feedback.

Lastly , I am indebt to my friends, my sister and my parents for their encouragement and support, specially during times when I was being exceptionally difficult. Thank you for keeping your hopes and patience, when I lost mine.